The evolution of an individual-like dispersive stage in colonial siphonophores

Maciej K. Mańko[1*], Catriona Munro[2], Lucas Leclère [2,3]

Affiliations

[1] Laboratory of Plankton Biology, Department of Marine Biology and Biotechnology, University of Gdansk, Gdynia, Poland
[2] Sorbonne Université, CNRS, Laboratoire de Biologie du Développement de Villefranche-sur-mer (LBDV), Villefranche-sur-Mer, France
[3] Sorbonne Université, CNRS, Biologie Intégrative des Organismes Marins (BIOM), Banyuls-sur-Mer, France
*maciej.manko@ug.edu.pl

Abstract

Evolutionary transitions between individual and colonial organisms remain enigmatic. Siphonophores, abundant pelagic cnidarians, exhibit a complex colony structure composed of repeated individual (zooid) clusters called cormidia. Many siphonophores release their posterior-most cormidia as independent fragments known as eudoxids, ensuring sexual reproduction. However, the mechanisms of eudoxid production and its evolutionary origins are unknown. Using live imaging, immunohistochemistry and pharmacological inhibition we provide a mechanistic understanding of eudoxid formation. We demonstrate that eudoxid release is controlled by a dedicated muscle and involves tissue remodeling, leading to the formation of an integrated dispersive unit with specific behaviors and a different buoyancy. We show that eudoxids and parental colonies often have different spatial or temporal distributions, suggesting niche partitioning. We infer that eudoxids evolved once through the concomitant evolution of multiple cormidium subparts. This study reveals how the acquisition of an individual-like dispersal stage, through muscle evolution and colony modification, contributed to the ecological success of a primary carnivore in marine planktonic ecosystems.

Teaser

Co-option of a muscle in siphonophores enabled life cycle complexification and ecological diversification

Introduction

The hierarchical integration of lower-level entities into higher-level units of selection has led to some of the most remarkable cases of biological evolution, from multicellular aggregations of cells, to colonial or social aggregations of individuals (1-3). As the integration progresses, lower level units may specialize and their individuality may become subordinated (4). In clonal colonial animals, such as hydrozoans (Cnidaria), this evolutionary transition in individuality has been likely achieved by retention of asexually budded individuals, driving subsequent division of labor and polymorphism of colony-building modules (5), followed by an evolutionary complexity drain (decreased complexity of a module compared to its free-living counterpart; 6). Such functional diversification of modules, integrated to jointly perform as a single organism, blurs the distinction between the individual and the colony.

Clonal colonial organization, in which genetically identical individuals (called zooids, ramets, etc.) remain physiologically integrated, offers multiple ecological advantages, derived from their modularity and unconstrained growth (e.g., 7 and references therein). One notable advantage is the ability to escape senescence by simply removing or replacing a malfunctioning building-block of a colony (8). Almost 50% of animal phyla exhibit some form of agametic reproduction, often leading to colony formation (6). While such organization arises, the evolutionary conflict unfolds. The reproductive duality between modules proliferating asexually and colony reproducing sexually may drive selection-based evolutionary tension, ultimately leading to colony becoming the primary unit of selection (9). Additionally, the population structure of colonial species, and thus their trait heritability, can vary significantly based on their dispersion strategies (10).

Dispersal capacity plays an important role in the ecological and evolutionary success of colonial organisms (11). Many colonial animal species are sessile hermaphrodites (e.g., 12-13), a favorable trait for colonizing adjacent habitats (13), but it limits long-range dispersal and may lead to inbreeding depression (14). To overcome these challenges, most colonial species have evolved a complex life cycle with a dispersive stage either before fertilization (a reproductive individual released from the colony) or after (planktonic larvae), enhancing their ability to disperse over longer distances despite their sedentary lifestyle. However, not all colonial taxa are sessile, with planktonic colonies found in two animal phyla: Chordata (salps, doliolids and pyrosomes) and Cnidaria (siphonophores). Despite their morphological diversity, all planktonic colonies share a number of traits, likely shaped by the dynamic pelagic environment (4). Unlike their benthic counterparts, planktonic colonies are motile, moving with sophisticated multi-jet systems (e.g., 15), and are characterized by directional growth with limited plasticity and branching (4). Pelagic colonial taxa are also known to have broader distributional ranges, as compared to their benthic counterparts (16). In spite of their great motility, many pelagic colonial species still display complex life cycles, the ecological and evolutionary significance of which remain to be studied.

Siphonophores, a clade of entirely marine hydrozoan cnidarians, have unequivocally the most complex colony architecture and the highest degree of zooid functional specialization among animals (17). The majority of siphonophore colonies are streamlined, with asexual budding of zooids restricted to either one or two localized growth zones (17). Budding follows a species-specific pattern, resulting in an iterative cluster of polymorphic zooids, called cormidia, dispersed along an elongated stem that plays a role in coordination and resource sharing between zooids (4, 18). Siphonophore

zooids (see Box of terms) are thought to be homologous to free-living polyps and medusae, although they have undergone substantial morphological simplification following functional specialization. Despite limited data on siphonophore reproduction and life cycles (19), siphonophores are known to decouple sexual reproduction from parental colonies, by detaching gonophores (i.e., medusa-like zooid) bearing gonads, either individually or in clusters (gonodendra detachment in *Physalia*, 20), similar to medusae release in other hydrozoans (Fig. 1A, B). After detachment, gonophores swim away from the parental colony and release gametes, which after fertilization will give rise to planula larvae (Fig. 1; 19). As gonophores are incapable of feeding, they only have a limited dispersal capacity.

Some members of the most-speciose clade of siphonophores, Calycophorae, took reproduction related specialization one step further. Instead of releasing a gonophore, which is merely a motile storage container of mature gametes, their colonies undergo evolutionarily unique, sequential fragmentation, releasing entire zooid clusters, called eudoxids (Fig. 1C). The eudoxids show distinct morphology, compared to cormidia still attached to the colony. This has led earlier authors to consider them as belonging to different species (reviewed in 21), mirroring how the medusa stage in other hydrozoans was often described under a different specific name than the polyp colony it originated (22). The realization that eudoxid is a life cycle stage and not a separate species came in 1853, from two independent studies (23-24). Nevertheless, new “eudoxid species" continued to be described, under the genus *Eudoxia* (25), awaiting the taxonomic identification of their potential parental colony (26).

The organismal nature of eudoxid is puzzling (e.g., 27). If assessed by their multi-zooid composition, they can be referred to as a colony, originating from another colony, a view supported by numerous authors (e.g., as monogastric colonies, 28). Alternatively, eudoxids could be considered akin to individuals, similar to how siphonophore polygastric colonies are often referred to as superorganisms (29). However, for eudoxids to qualify as individuals, their components would need to demonstrate sufficient physiological and functional interdependence to operate as an autonomous, integrated unit capable of persisting over time, reproduction, and effective selection (3, 30-31). However, evidence supporting these criteria is largely missing.

Despite over two centuries of siphonophore research (18), the mechanisms of eudoxid production, its ecological significance and evolutionary history remain unknown. To the best of our knowledge, the sole attempt at describing the process of eudoxid release (31), mentioned only the narrowing of stem at weak points and the subsequent deterioration of the stem that connects the posterior-most cormidium to the rest of the colony, and concluded that the process is spontaneous. All other accounts of the process pertained to its speed, linking it with water temperature and food availability (32). To properly describe this individual-like stage in the siphonophore life cycle, we first characterized eudoxid production using in vivo imaging, immunohistochemistry, electron microscopy and pharmacological inhibition experiments. We then assessed its ecological significance by reviewing the entirety of siphonophore literature, and placed it within an evolutionary framework by improving the calycophoran phylogeny with a broader taxon sampling and conducting morphological character evolution analyses.

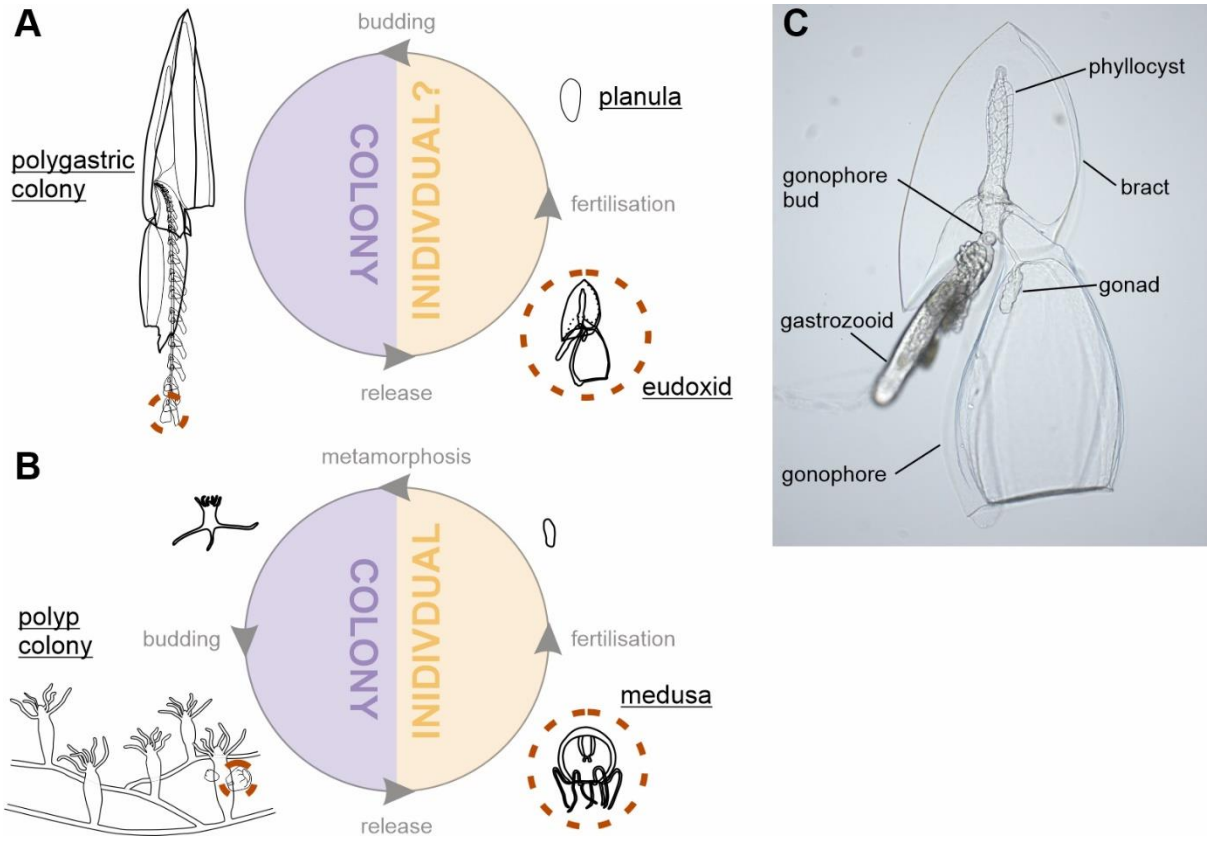

Fig. 1. Life cycle stages of Calycophoran siphonophores.

Life cycle of a calycophoran siphonophore, *Chelophyes appendiculata* (**A**), and a non-siphonophore cnidarian *Podocoryne carnea* (**B**), with major processes in light gray and individual-colony transition distinguished with colors. (**C**) Morphology of *C. appendiculata* eudoxid stage.

Box of terms. Siphonophore-specific terminology

Bract – gelatinous zooid likely required for buoyancy and defense.
Bracteal canal – diverticulum of gastrovascular system into the bract. Primary branch called a longitudinal canal, and subsequent branches may be present.
Cormidium – reiterating sequence of zooids found along the stem.
Eudoxid – stage in life cycle of some Calycophorae; detached cormidium of polygastric colony.
Gastrozooid – feeding zooid, homologous to polyps.
Gonophore – reproductive zooid, homologous to medusae.
Nectophore – swimming zooid, homologous to medusae.
Phyllocyst – swollen branch of bracteal canal system in eudoxids.
Polygastric colony – stage in Calycophorae life cycle, comprising nectophore(s) and zooids arranged along stem.
Somatocyst – swelling of gastrovascular canal within nectophore tissues.
Stem – longitudinal stolon, to which zooids are attached.
Stem fragments – free-living stem fragments, likely arising through mechanical injury to colony.
Zooids – functionally specialized, colony building blocks/units, arising through incomplete budding.

Results

Stages of cormidium development

Eudoxid formation was characterized in *Chelophyes appendiculata*, a highly abundant, epipelagic siphonophore species, known to release eudoxids (33), whose ease of collection permitted extensive observations. The process comprises three spatially and temporarily separated processes: cormidium development, cormidium release and eudoxid maturation, of which the latter occurs only in released cormidia. Cormidia, the iterative clusters of zooids, are budded off in a fixed anterior location, called the growth zone, and then develop gradually, carried posteriorly via stem extension (Fig. 2). The pace of cormidium development is not a function of stem length, as cormidia of all stages can be found in specimens with short stems. Four distinct stages of cormidium development can be distinguished based on differences in size and morphology of bract and gonophore. Newly budded cormidia initially appear as an undifferentiated projection from the stem, a probud (17), that first develops into a gastrozooid (Fig. 2B, E), hence entering into stage 1 (S1) of cormidium development. As the gastrozooid enlarges and its tentacle develops, the bract buds off from the left-hand side of the gastrozooid's peduncle (see 34 for siphonophore axes; Fig. 2A, B, C, E). Actin-rich structures can be seen at the base of the bracteal canal (Fig. 2C), whose presence in other connection sites (e.g., stem-nectophore, Fig. S1) in *C. appendiculata* colony suggest their role in attachment. The bract, initially a minute, shield-like zooid covering gastrozooid's base, progressively extends over the stem migrating towards the stem's dorsal side (Fig. 2A, B), while the bracteal canal elongates to eventually become positioned perpendicularly to the anterior-posterior axis of the stem. The migration of the bract stops when the central portion of the bracteal canal is opposite to the gastrozooid, and this coincides with the appearance of a gonophore bud from the left-hand side of the gastrozooid's peduncle, marking the end of stage 1 (S1) of cormidium development (Fig. 2E, F). As development progresses, the bract enlarges and the gonophore becomes more prominent (Fig. 2F). The bracteal canal, originally a tubular structure embracing the stem, develops an apical projection, marking the transition into stage 2 (S2) of cormidium development (Fig. 2F, I). At this stage, the bract resembles a cone wrapped around the stem, so that the right side overhangs the left one (Fig. 2F). When the apical projection of the bracteal canal grows twice as tall as its lateral branches, the cormidium enters stage 3 (S3) of development (Fig. 2G). At this stage, the gonophore becomes more differentiated and starts pumping actively. The bract's shape does not visibly differ from the bract at S2. During the transition into stage 4 (S4; Fig. 2H, I), the lateral branches of the bracteal canal retract, while its apical projection enlarges and protrudes deeper into the bract, likely due to the mesoglea build up in the surrounding tissue (Fig. 2H). As a result, only two connections between the bracteal canal and the stem are maintained: the apical, joining the bracteal canal's apical projection with the stem, and the basal. Simultaneously, the bract shortens and acquires a more triangular shape than in S2 or S3; in addition, the two flaps of the bract retreat revealing bracteal furrow, the groove that the stem runs through (Fig. 2H).

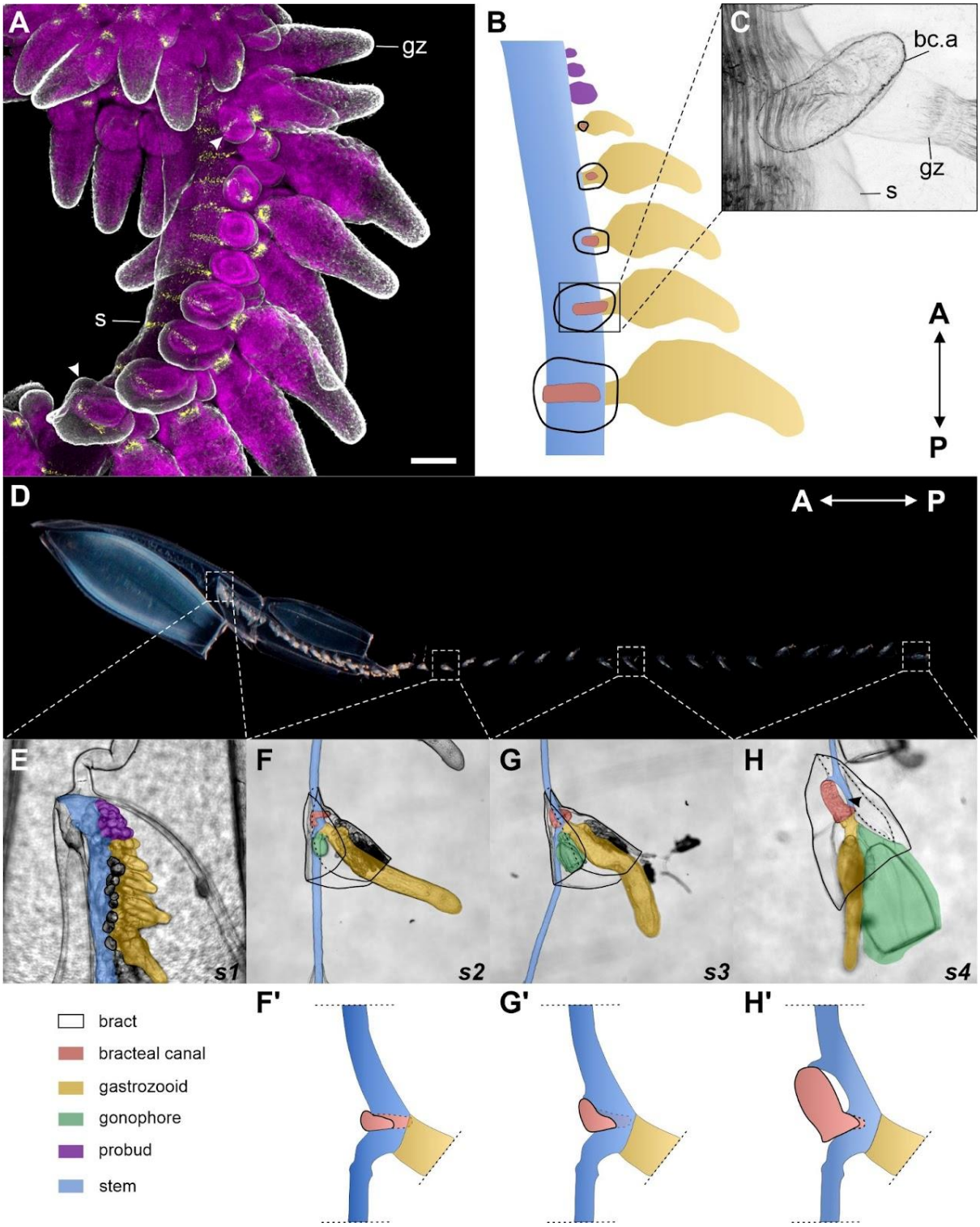

Fig. 2. Stages of cormidium development in *Chelophyes appendiculata*.
A. Immunohistostaining of tyrosinated tubulin (grey), FMFRamide (yellow) and nuclei (magenta) in young *C. appendiculata* stem. Arrowheads point at the youngest (top = anterior) and the oldest (bottom = posterior) bract visible. Scale bar: 100 µm. **B.** Schematic representation of early cormidium differentiation with color-coded zooids. **C.** Actin detection in young stem showing junction of bracteal canal and the gastrovascular system of a gastrozooid. **D.** Overview of *C. appendiculata* colony. **E.–H.** Stages S1–S4 of cormidium development, with color-coded zooids and other components of the colony.

Black arrowhead points at the mesoglea build up site between the bracteal canal and the stem. **F', G', H'.** Schemes of bracteal canal progression through stages S2 (F), S3 (G) and S4 (H), with the extent of stem and gastrozooid limited by the dashed line; note that the H photo shows terminal S4 cormidium, while the corresponding scheme (H') documents S4 cormidium morphology in precedent cormidium (*i.e.*, not terminal). Figures are aligned so that the anterior pole of the colony faces up, except for D., where the colony's anterior pole faces left. Note that figures: A, B, C, E were flipped for presentation purpose, and that in all schemes gastrozooid's tentacles were omitted for clarity. Labels: bc.a – bracteal canal attachment, gz – gastrozooid, s – stem.

Disruption of connectivity between cormidia triggers their ordered release

Earlier attempts at characterizing cormidium release in actively moving colonies in the Petri dish proved unsuccessful, as colonies would fragment randomly upon swimming into the walls of the dish. Only after immobilizing nectophores (N = 8 colonies; for details see Methods) or placing colonies in large containers (N = 2), were we able to document (N = 20 observations; 2 release events per each of 10 colonies; Table S1), that cormidia are always released one-at-a-time (20/20), consistently upon reaching S4 of development (14/14; staging not performed in 6 cases), and in a fixed order, starting from the posterior end of the colony (20/20 cases).

We also found that cormidium release can be triggered by disrupting the connection between a stem fragment with several cormidia and the remaining colony (Table S2). 2-, 3-, and 4- cormidia-long stem fragments (CLSF) at S3 of cormidium development (N_{CLSFs} = 1, 8, 7, respectively) dissected off from *C. appendiculata* colonies consistently released all their cormidia ($N_{released\ cormidia}$ = 56). With only a single exception (Movie S1), the release progressed anteriorly from the posterior-most cormidium. Interestingly, when a stem of a single colony was cut into two 3-CLSFs ($N_{colonies}$ = 6), the order of cormidia release was maintained within each fragment, but not between the two fragments i.e., the two fragments started releasing posterior-most fragments nearly simultaneously, implying release inhibition by the presence of the posterior cormidia.

Muscle contraction at the detachment ring is involved in cormidium release

To characterize the sequence of events leading to the cormidium release, we designed an experiment, in which 3-CLSFs were locked in position using a glass micro-chamber and were then filmed over an extensive period of time. Analysis of frame grabs revealed that the release of cormidia is preceded by a constriction of the stem at a specific site, henceforth called detachment ring, immediately posterior to the gastrozooid's peduncle of a second-to-last cormidium of the colony (Fig. 3A, B, Movie S1). While the detachment ring remains constricted, the posterior portion of the stem undergoes a series of longitudinal contractions, and the gonophore continues to pump, ultimately leading to the release of the terminal cormidium at the detachment ring. The detachment ring remains constricted even after the release, as indicated by actin staining (Fig. 3D, E), and gets resorbed by the preceding cormidium only later (Fig. 3F). This likely serves to maintain separation of the gastrovascular system from the surrounding environment.

The muscular nature of the detachment ring was corroborated by transmission electron microscopy (Fig. 3C'-C'''). The detachment ring is made up of two layers of myofilaments, as indicated by the hexagonal lattice of myosin and actin filaments (Fig. 3C'''): ectodermal and endodermal, separated by an electron dense layer of mesoglea (Fig. 3C', C'''). On the ectodermal side, mesoglea branches out, separating individual

myofilaments, likely to provide additional support, while no such branching was observed on the endodermal side. Importantly, the two layers of myofilaments are perpendicular to each other (Fig. 3C’’’), with the ectodermal layer running along the stem's length, while the endodermal layer forms circular bands within stems’ lumen. In contrast to the detachment ring, the surrounding stem does not contain the endodermal muscle layer, and the ectodermal layer appears thinner (Fig. 3C’’).

To further test the role of muscles in cormidium release, we performed a series of pharmacological inhibition experiments on 2- and 3-CLSF, blocking either muscle contractions (isotonic $MgCl_2$ solution) or myosin II activity (Blebbistatin in DMSO; Table S3). In control conditions (MFSW-control and DMSO-control stem fragments), the release was relatively rapid, always resulting in the appearance of fully-formed eudoxids within 22h. Treatment with non-muscle myosin inhibitor slightly impaired stem’s ability to release cormidia, more pronouncedly at higher concentrations (release success of 71.43% and 35.71%, for 1 μM and 5 μM Blebbistatin, respectively), while blocking with magnesium chloride consistently impaired stem’s ability to release cormidia (success rate 4.5%).

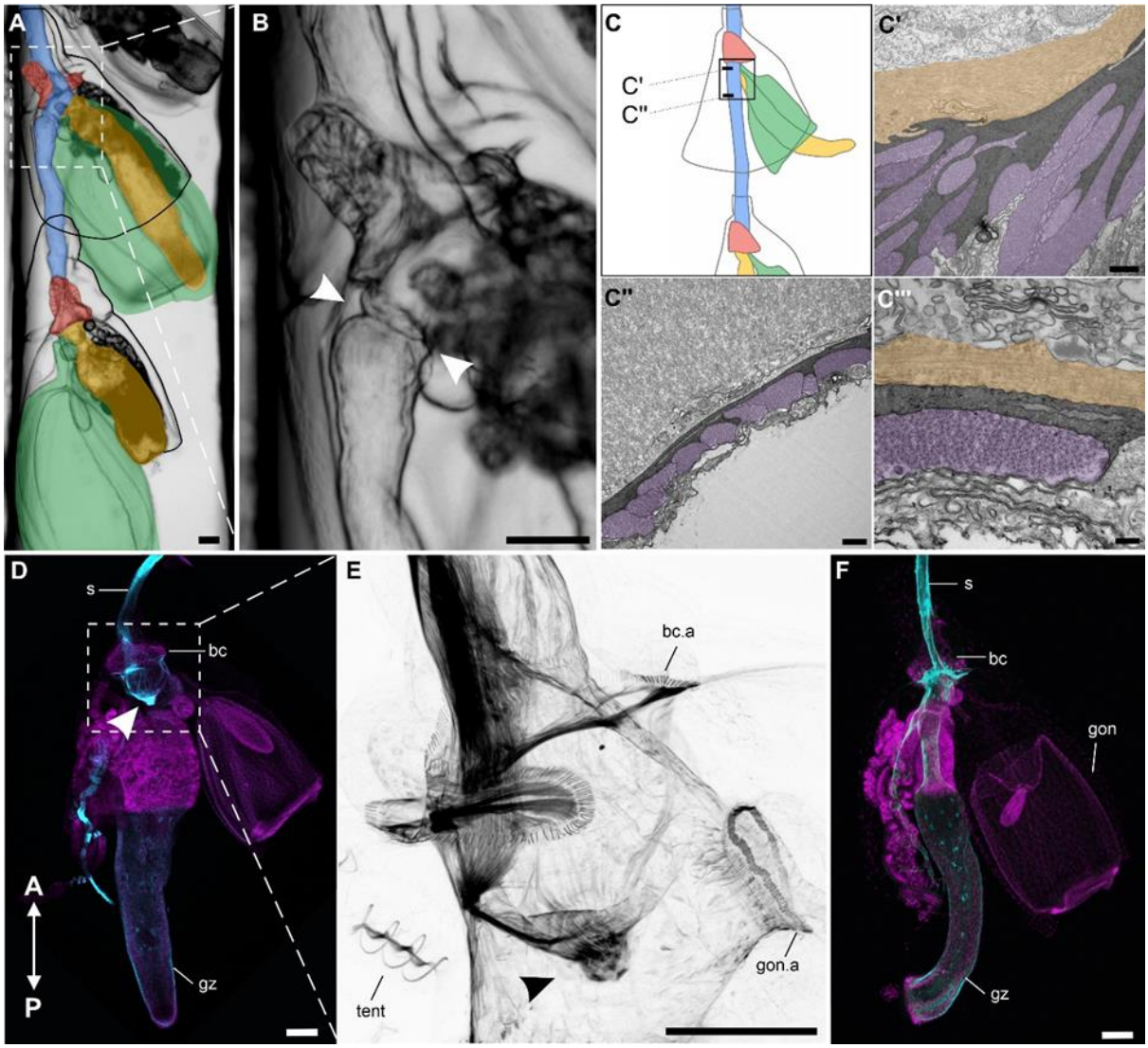

Fig. 3. Constriction at the detachment ring is necessary for cormidium release. **A.** A three-cormidia-long stem fragment (from Movie S1), with a constricted detachment ring at the second-to-last cormidium. Color coded as in Fig. 1. **B.** Close-up of the detachment ring showed in (A). **C.** Schematics of TEM ultra-thin sections shown in panels C' and C''. **C'**. Microanatomy of the detachment ring, with endodermal muscle myofilaments colored in orange and their ectodermal counterparts in purple. **C''.** Stem microanatomy below the detachment ring, color scheme as in C'. **C'''.** Close-up of myofilaments across mesoglea within the detachment ring. **D.** Actin (cyan) and nuclei (magenta) detection in the second-to-last cormidium fixed right after the detachment of the posterior-most cormidium. **E.** Close up of the area marked in (D), depicting a constricted detachment ring (arrowhead) and the actin-rich structures associated with attachment sites (Fig. S1). **F.** Actin (cyan) and nuclei (magenta) detection in the posterior most cormidium without any visible remnants of the detachment ring. All figures are aligned so that the anterior pole of the colony faces up. Labels: bc – bracteal canal, bc.a – bracteal canal attachment, gon – gonophore, gon.a – gonophore attachment, gz – gastrozooid, s – stem, tent – tentillum, arrowhead: detachment ring. Scale bars: 100 μm (A, B, D, E, F), 1 μm (C', C''), 200 nm (C''').

Cormidium competence to release arises with development of bracteal canal and detachment ring

Our initial observations indicated that *C. appendiculata* colonies with less developed stems did not produce eudoxids (Table S1). To systematically test if this ability correlates with cormidium maturation we dissected 2-, 3- and 4-CLSFs (N_{CLSFs} = 3, 16, 12, respectively) at S2 of development (Table S2). Of the 102 S2 cormidia in 31 stem fragments none were released throughout the duration of experiment, thus indicating that the competence to release arises during transition from S2 to S3 of cormidium development. Interestingly, during this assay bracts detached from all cormidia within the first 24 h of the experiment, suggesting weaker bract-stem attachment at this stage of cormidium development.

Through detection of actin and nuclei in *C. appendiculata* stems we were able to associate the competence to release eudoxids with the development of the detachment ring and bracteal canal. The detachment ring is already discernible in cormidia within the growth zone (Fig. 4A, A'), and is directly associated with the newly budded gastrozooids, *i.e.*, a single detachment ring form posteriorly to each gastrozooid. At first, the detachment ring has a form of a semi-ring, made up of few myofilaments running perpendicularly to the A-P axis of the stem, extending from gastrozooids' base, to roughly mid-width of the stem on both sides of the gastrozooid (Fig. 4A, A'). As the cormidium develops, the detachment ring begins to encircle the entire stem whilst remaining being made up of few, relatively thin myofilaments (Fig. 4B, B'). Then, upon entering S3 of cormidium development, the detachment ring migrates posteriorly, its longitudinal extent increases, the circular muscle bands widen (Fig. 4C, C'), and so does the overlying ectoderm, hence rendering the detachment ring distinguishable even without the actin staining (Fig. 4D). Similarly, the bracteal canal development (Fig. 1A, E-H) appears to be associated with the strengthening of the bracteal canal and stem connection, as indicated by actin detection (Fig. 4) and the S2 dissection experiment (see precedent paragraph).

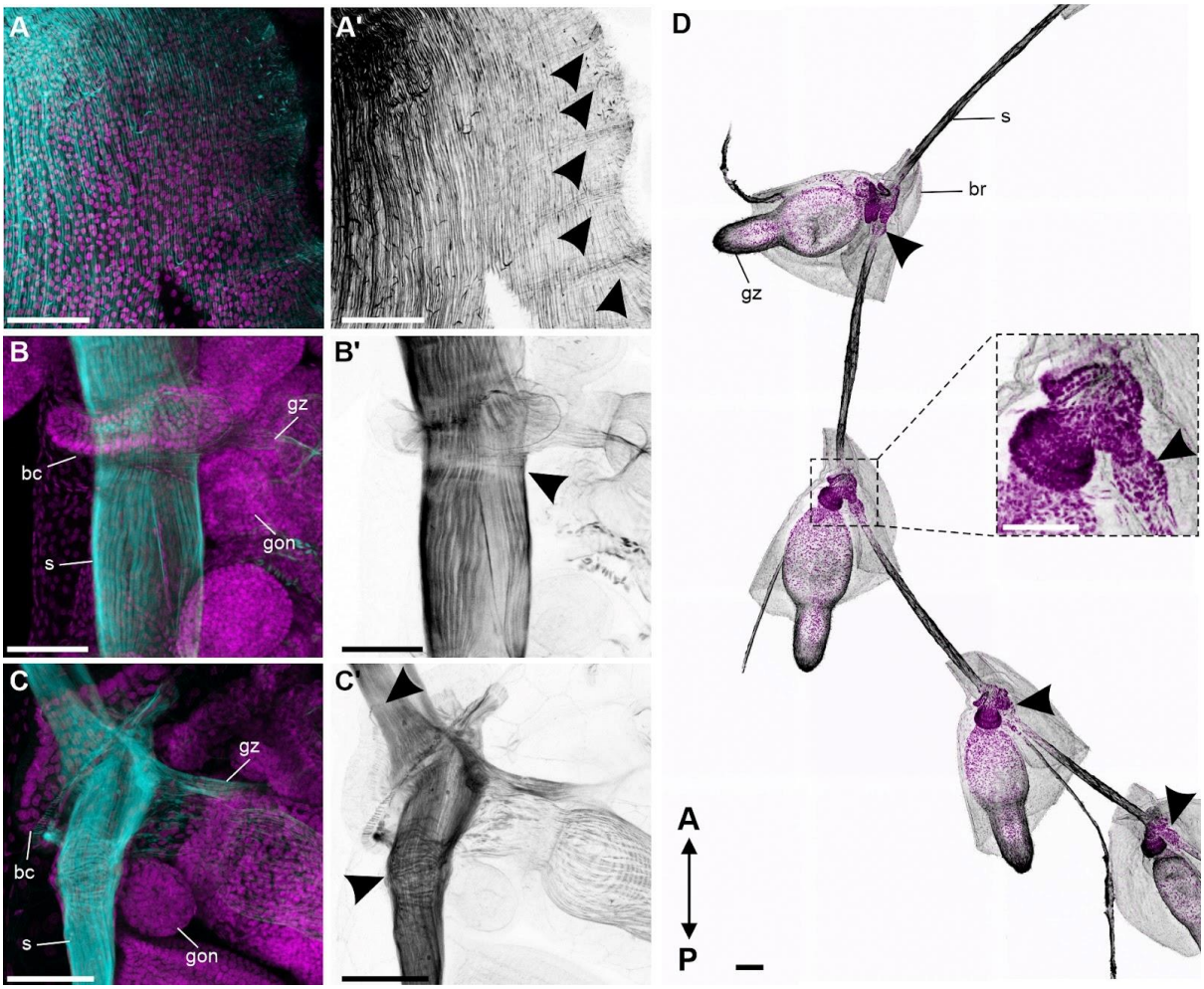

Fig. 4. Detachment ring and stem-bracteal canal connection change during cormidium maturation.
Actin (cyan in A, B, C, grey in A', B', C') and nuclei (magenta) detection in the colony of *C. appendiculata.* **A. A'.**growth zone, **B. B'.** S2 cormidium, **C. C'.** S3 cormidium. Arrowheads point at the developing developing detachment rings (A, B,C). **D.** Tyrosinated tubulin (gray) and nuclei (magenta) detection in *C. appendiculata* stem with four S3 cormidia with a close-up of one of detachment rings (inset). Arrows point at detachment rings. A-P depicts anterior and posterior axis in all figures. Labels: bc – bracteal canal, br – bract gon – gonophore, gz – gastrozooid, s -stem. Scale bars: 100 µm.

Cormidium release induces eudoxid maturation
The process of release triggers eudoxid maturation, during which the bract develops a distinct morphology (Fig. 1C, 5). To reconstruct the course of post-release maturation, we again exploited time lapse videos (Fig. 5A, Movie S1-S3). The newly released cormidium always possessed an elongated piece of stem, which it will later resorbed, so that within c. 2h the only visible remnant of the stem was associated with the stem-bracteal canal connection sites (Fig. 5A). Only after that connection was broken the stem resorbed completely (Fig. 5E, F). Likewise, the preceding cormidium's remnant of the stem with the detachment ring (Fig. 3D) also become resorbed (Fig. 3F).

During stem resorption, the bracteal canal elongated, simultaneously narrowing down, and started protruding deeper into the mesoglea, marking the formation of a phyllocyst (Fig. 5A). This occured concomitantly to a tilt in the anterior-posterior (A-P) axis of the

eudoxid. In the *C. appendiculata* colony, the stem sets the A-P axis, so that the bracteal canal is positioned perpendicularly to it (Fig. 1A-E). The apical projection of the bracteal canal, arising during cormidium maturation, develops at the angle to the colony's A-P axis (Fig. 2A-E). Then, after the release, the longer axis of the eudoxid's phyllocyst becomes the A-P axis of the eudoxid (Fig. 5A).

The most apparent component of the eudoxid maturation is bract remodeling. The primary difference, when comparing newly released eudoxid to the mature one, lies in the volume of bract, that increased post-release (Fig. 5A). Since the entirety of our experiments have been run on 1-day-starved specimens in microfiltered seawater, the lack of potential nutrition suggests that the volume increase is driven by the passive uptake of water by the mesoglea. This volume increase led the bracteal furrow to enclose, which in turn lad the bract's shape to change from the thin, leaf-like structure wrapped around the stem into a pyramidal one positioned on top of the eudoxid.

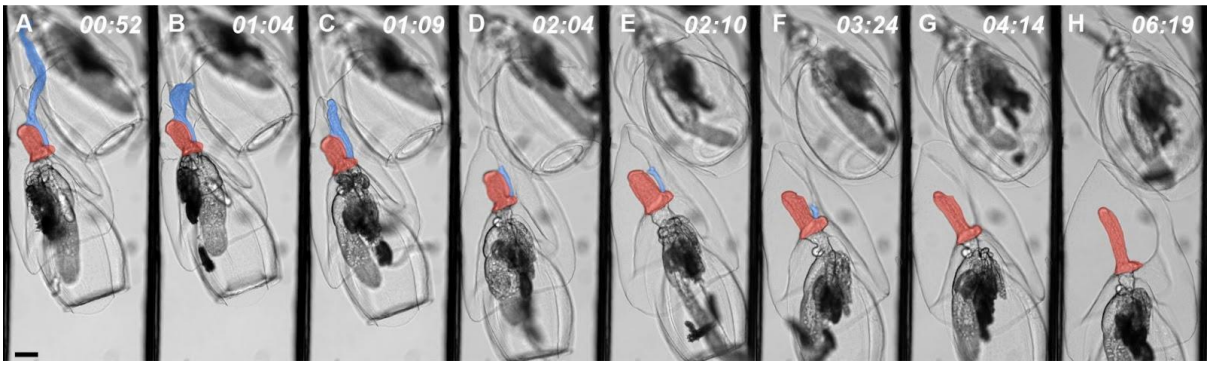

Fig. 5. Eudoxid maturation comprises stem resorption, phyllocyst formation and bract remodeling.
Individual frame grabs (**A-H**) with their timestamps (in hours after dissection) from time-lapse video depicting post-release modifications to cormidium morphology. Stem and bracteal canal/phyllocyst colored as in Fig. 2. Scale bar (shown only in A): 100 μm.

Eudoxid maturation is actomyosin dependent

The active nature of stem resorption, together with the existing data on the role of actomyosin in shape acquisition in Medusozoa (e.g., 35), prompted us to investigate the control mechanisms of eudoxid maturation. Following the release of a cormidium, the stem undergoes a series of contractions (e.g., Fig. 5), likely facilitating the resorption, which appear dependent on the stem-bracteal canal connection site (Fig. 6A, B). Strong actin signal from that area in maturing cormidia (Fig. 6A, B) indicates that it is the site of active pulling of the stem remnant. In a eudoxid with a fully resorbed stem, the traces of stem-bracteal canal connection are gone, with the base of phyllocyst formed by circularly arranged actin-rich structures (Fig. 6C; Fig. S1).

In contrast, the lack of actin detection on the bract's surface and a faint actin signal within the bracteal canal (Fig. 6A, B), imply that their shape changes are not achieved by spatial differences in the surface tension, but are likely myosin-dependent. To further test this, we returned to the previously mentioned pharmacological inhibition experiments and scored the resulting phenotypes (Fig. 6D-H, Table S3). Treatment with a well-known anesthetic (magnesium chloride) did not affect bract remodeling, with only 13.64% cases of bracts with aberrant morphology (Fig. 6D). Similarly, the development of bracteal canal appeared unaffected, with just 22.73% cases of retained apical connection with bract's

surface (as in Blebbistatin treatment). Interestingly, although cormidium detachment was not observed, connected cormidia appeared to begin resorbing adjacent stem leading to its extreme narrowing (Fig. 6D,H). As a result, a 3-CLSF in magnesium chloride treatment would go through every stage of cormidium development and eudoxid maturation, but would remain interconnected through a narrow stem.

Treatment with non-muscle myosin inhibitor uniformly led to malformed bracts (N = 28) and bracteal canals (N = 28; Fig. 6D). Bracts in Blebbistatin-treated stem fragments continued to grow but failed at remodeling, which resulted in their pronounced flattening (Fig.6F). Bracteal canals expanded, as during progression from S3 to S4 of cormidium development, but failed to elongate, rather forming a more oval structure. In addition, the bracteal canal in released cormidia remained connected with the bract's surface through the apical connection, hence bending towards the direction of the bracteal furrow (Fig. 6F, G). The stem resorption was also affected, as remnants of stem could have been discerned both along the bracteal furrow and near the bracteal canal base (Fig. 6G).

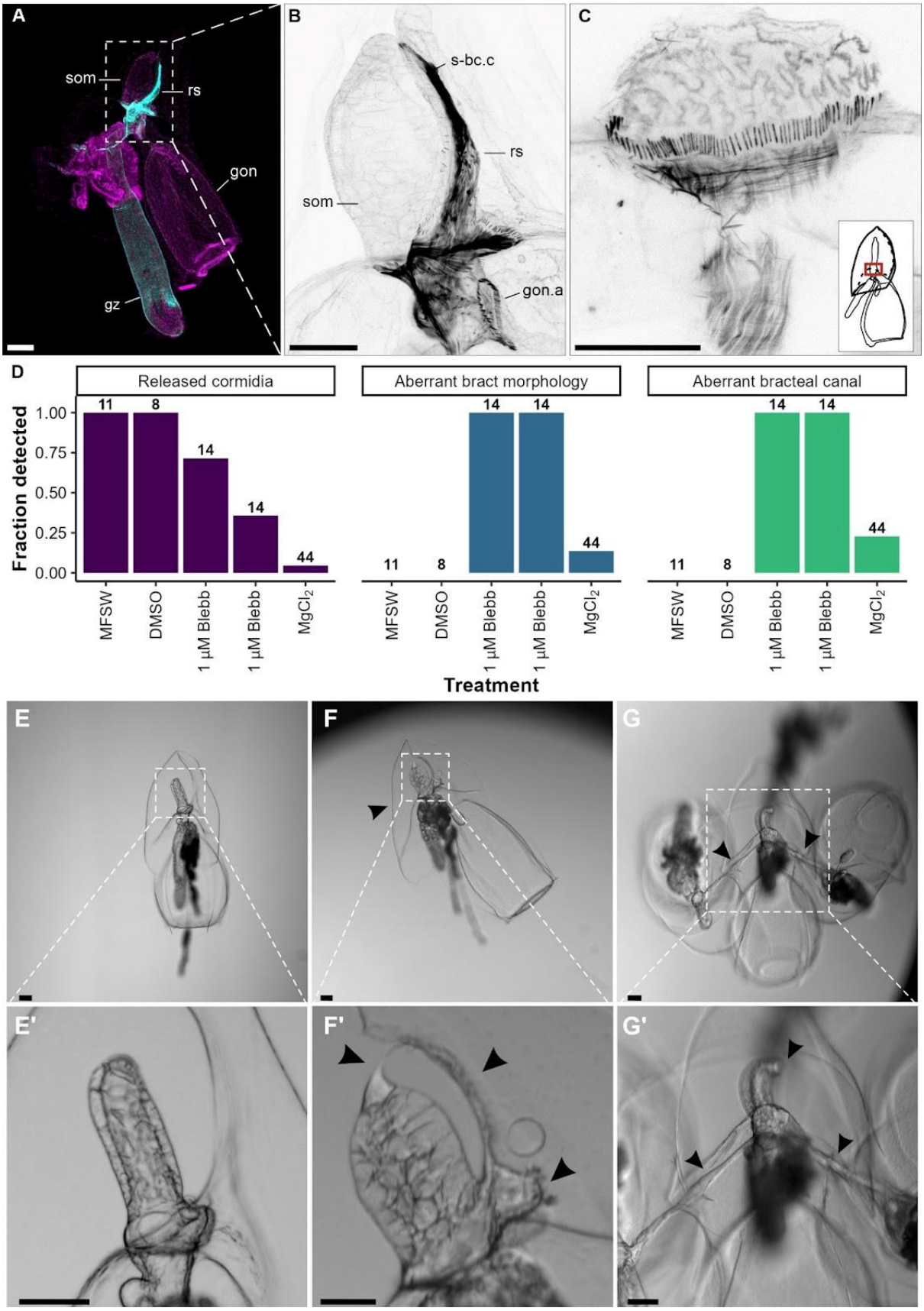

Fig. 6. Cormidium release and eudoxid maturation depend on muscle activity.
A. Actin (cyan) and nuclei (magenta) detection in newly released cormidium. **B.** Close up of A. depicting actin detection in stem-bract connection site. **C**. Actin detection at the base

of mature eudoxid phyllocyst – red rectangle on the inset marks the location of the close up. **D.** Results of a pharmacological inhibition experiment scoring released cormidia, aberrant bract morphology and aberrant bracteal canal morphology across treatments with number of observations per treatment shown in bold (Table S3; MFSW - microfiltered sea water, DMSO, 1µM Blebb - Blebbistatin in DMSO, 5µM Blebb - 5µM Blebbistatin in DMSO, isotonic $MgCl_2$- isotonic 7.5% $MgCl_2$ solution in MFSW). **E.** Normal phenotype of eudoxid from control MFSW treatment. **E'.** Close up of E showing phyllocyst morphology. **F.** Eudoxid with flattened bract (arrow) from 5µM Blebbistatin treatment. **F'.** Close up of F showing un-resorbed stem (right-hand arrows) and aberrant phyllocyst, connected with bracteal furrow (arrow on the left side). **G.** Three cormidia from $MgCl_2$ treatment remaining interconnected with narrow stem (arrows), each with remodeled bract and some aberrations to phyllocyst formation. **G'.** Close up of G with arrows pointing at narrow stem (left and right arrow) and bent phyllocyst (top arrow). Scale bars: 100 µm, except for C where scale bar is 50 µm.

A single acquisition of the eudoxid in calycophoran siphonophores

Our phylogenetic analyses provided a comprehensive picture of the evolutionary relationships within Calycophora, thanks to the acquisition of new 16S and 18S sequences for previously unsampled species and genera (notably Clausophyes, see Fig. 7A, Table S5). This robust phylogeny, constrained on a phylogenomic backbone (36, see Methods), allowed us to propose a taxonomic revision of Calycophoran families. We propose to dismiss the family Abyliidae as it is nested within Diphyidae. Since the family Clausophyidae appears polyphyletic, we propose to split it into two groups based on whether the genera produce eudoxids or not: (1) Chuniphyidae fam. nov., which contains the type genus *Chuniphyes* Lens & van Riemsdijk, 1908, as well as the other eudoxid-producing genera *Crystallophyes*, *Kephyes*, and *Heteropyramis*; and (2) the revised family Clausophyidae Totton, 1965, now including only one genus, *Clausophyes*, which does not produce eudoxids. The new clade Eudoxida, defined by the presence of a eudoxid in the life cycle, includes the families Chuniphyidae, Sphaeronectidae, and Diphyidae. The inclusion of *Tottonophyes enigmatica* in this clade remains ambiguous, awaiting confirmation that it produces eudoxids, as suggested by Pugh et al. (37). The revision of the paraphyletic family Prayidae will await future studies, as sequences were missing for many prayid species.

By reconstructing 26 characters on the phylogeny (Data S1), we inferred a unique acquisition of the eudoxid in the common ancestor of Eudoxida, following a stepwise acquisition of the different structures that compose the eudoxid-producing cormidia. In all described species, eudoxids are composed of a unique bract, a gastrozooid, and a gonophore, which are all part of each cormidium. These structures were present in the common ancestor of physonect and calycophoran siphonophores, with the cormidia becoming simplified in the common ancestor of calycophorans, notably with only one bract and one gonophore per cormidium, the latter being attached at the base of the gastrozooid. The canal structure of the bract was then simplified within Eudoxida, in the clade sister to Chuniphyidae. We further inferred a single loss of the eudoxid, in the ancestor *Sulculeolaria*, as well as a loss of the bract in the common ancestor of Clausophyidae and Hippopodiidae. The ability of some prayid species to fragment their stem could not be linked to the origin of eudoxids, as this characteristic was found scattered among non-Eudoxida calycophores.

The single acquisition of the eudoxid in the common ancestor of Eudoxida coincided with the acquisition of a several characters: the phyllocyst, the ability to release cormidia, the bract's ability to change morphology when detached, and the change in the angle of longitudinal canals, which became perpendicular to the stem. To be released, eudoxids need the presence of a detachment ring (Fig. 7B), a structure which we inferred to be a synapomorphy of the clade Eudoxida. We could detect a detachment ring in the stem of five Eudoxida species investigated (Fig. 7B, *C. appendiculata*: Fig. 3), while a 'break' in the longitudinal fibers was observed at the corresponding location in four non-Eudoxida species (Fig. 7B). Further investigations in a broader set of species will be needed to confirm the origin of the detachment ring in the common ancestor of Eudoxida.

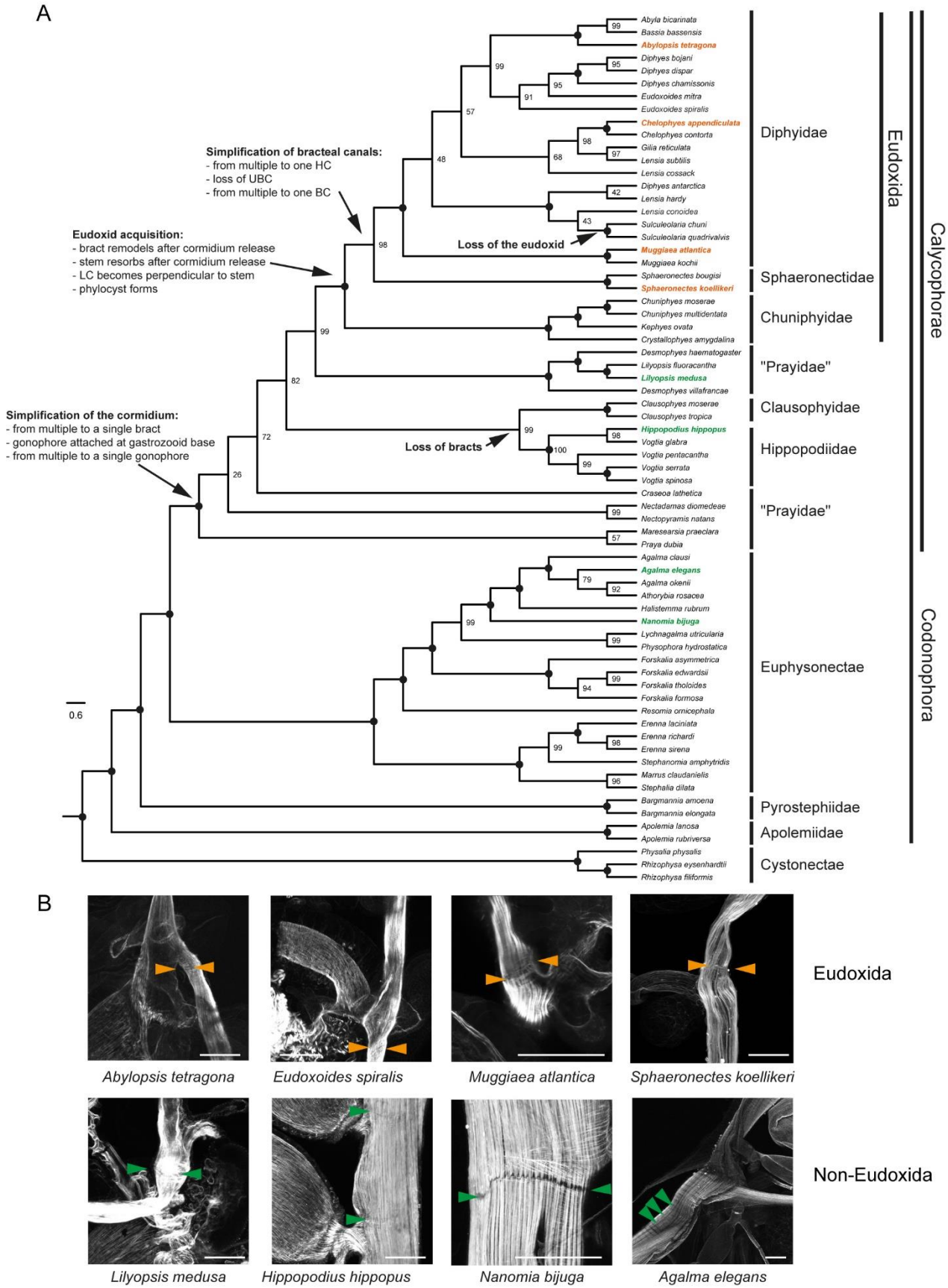
A
Simplification of bracteal canals:
- from multiple to one HC
- loss of UBC
- from multiple to one BC
Eudoxid acquisition:
- bract remodels after cormidium release
- stem resorbs after cormidium release
- LC becomes perpendicular to stem
- phylocyst forms
Loss of the eudoxid
Simplification of the cormidium:
- from multiple to a single bract
- gonophore attached at gastrozooid base
- from multiple to a single gonophore
Loss of bracts
0.6
Abyla bicarinata
Bassia bassensis
Abylopsis tetragona
Diphyes bojani
Diphyes dispar
Diphyes chamissonis
Eudoxoides mitra
Eudoxoides spiralis
Chelophyes appendiculata
Chelophyes contorta
Gilia reticulata
Lensia subtiliis
Lensia cossack
Diphyes antarctica
Lensia hardy
Lensia conoidea
Sulculeolaria chuni
Sulculeolaria quadrivalvis
Muggiaea atlantica
Muggiaea kochii
Sphaeronectes bougisi
Sphaeronectes koellikeri
Chuniphyes moserae
Chuniphyes multidentata
Kephyes ovata
Crystallophyes amygdalina
Desmophyes haematogaster
Lilyopsis fluoracantha
Lilyopsis medusa
Desmophyes villafrancae
Clausophyes moserae
Clausophyes tropica
Hippopodius hippopus
Vogtia glabra
Vogtia pentacantha
Vogtia serrata
Vogtia spinosa
Craseoa lathetica
Nectadamas diomedeae
Nectopyramis natans
Maresearsia praeclara
Praya dubia
Agalma clausi
Agalma elegans
Agalma okenii
Athorybia rosacea
Halistemma rubrum
Nanomia bijuga
Lychnagalma utricularia
Physophora hydrostatica
Forskalia asymmetrica
Forskalia edwardsii
Forskalia tholoides
Forskalia formosa
Resomia ornicephala
Erenna laciniata
Erenna richardi
Erenna sirena
Stephanomia amphytridis
Marrus claudanielis
Stephalia dilata
Bargmannia amoena
Bargmannia elongata
Apolemia lanosa
Apolemia rubriversa
Physalia physalis
Rhizophysa eysenhardtii
Rhizophysa filiformis
Diphyidae
Sphaeronectidae
Chuniphyidae
"Prayidae"
Clausophyidae
Hippopodiidae
"Prayidae"
Euphysonectae
Pyrostephiidae
Apolemiidae
Cystonectae
Eudoxida
Calycophorae
Codonophora
B
Eudoxida
Abylopsis tetragona
Eudoxoides spiralis
Muggiaea atlantica
Sphaeronectes koellikeri
Non-Eudoxida
Lilyopsis medusa
Hippopodius hippopus
Nanomia bijuga
Agalma elegans

Fig. 7. Siphonophore phylogeny based on 16S and 18S rDNA supporting a single origin of the eudoxid. A. ML phylogeny inferred from concatenated 18S and 16S sequences, constrained by the phylogenomic tree from Munro et al. (2018). Morphological evolution related to eudoxids is indicated on the phylogeny based on parsimony analysis. B. Actin (grey) detection in the stem for selected species shows a detachment ring in Eudoxida species (orange arrowhead), while a 'break' in the longitudinal fibers is observed at the corresponding location in non-Eudoxida species (green arrowhead). Scale bars: 100 μm.

Eudoxids and colonies display distinct spatiotemporal distributions

An extensive literature review allowed us to document differences in the distribution of eudoxids and polygastric colonies across scales (temporal, horizontal and vertical; Fig. 8) and species (Data S2). Although in the majority of cases, eudoxids were found to co-distribute with polygastric colonies, nearly 43% of references analyzed documented some sort of discrepancies in their distribution patterns.

Eudoxids were found to exhibit either broader (*Abylopsis tetragona*, 38, Fig. 8B) or narrower (*Muggiaea bargmanna*, 39) depth ranges than polygastric colonies (Fig. 8B). They would also often have non-overlapping vertical distribution with polygastric colonies, with examples of population structuring due to presences of thermoclines (*Muggiaea kochi*, 40). Eudoxids of certain species were found to occupy larger depths than the polygastric colonies (*Diphyes antarctica*, 41), while for others (*Gilia reticulata*, 41) the inverse was true.

Comparison of horizontal distribution of eudoxids and polygastric colonies revealed that despite their general similarity, they too may differ (Fig. 8A, D). Cases where eudoxids were present despite the absence of polygastric colonies were found both in localized studies (*Ceratocymba leuckartii*, 42) and those spanning greater oceanic regions (*Chuniphyes multidentata*, 43, Fig. 8C). These distributional differences often mirrored hydrological (*Heteropyramis maculata*, 44) and bathymetric (*Ceratocymba leuckarti*, 42) setting of the area, further supporting the idea of distinct distributions between eudoxids and polygastric colonies.

Although eudoxids are produced by polygastric colonies, suggesting their temporal distributions should be tightly coupled, we found evidence to the contrary (Fig. 8A, D). For example, we found that eudoxids could persist through periods of minimal or no presence of polygastric colonies (*Dimophyes arctica*, 46), implying extended lifespan of eudoxids and the ecological mismatch between the two. They were also found to associate differently with seasonal events, like the Northeast Monsoon (*Chelophyes appendiculata*, 42).

Surprisingly, eudoxids and polygastric colonies also exhibited a distinct diel pattern of distribution (Fig. 8A, E). This might have resulted from eudoxids not performing diel vertical migrations, contrary to polygastric colonies, or on the contrary, from eudoxids migrating more pronouncedly than polygastric colonies (*Ceratocymba sagittata*, 47).

Differences in vertical and diel distribution between eudoxids and polygastric colonies can be attributed to a unique buoyancy acquisition mechanism of eudoxids. As indicated in the previous section, eudoxid maturation involves pronounced volume increase of the bract, which renders eudoxids more buoyant compared to undetached cormidia. To compare the

buoyancy of the two, we designed an experiment in which stem of a starved colony, spanning all S3 and S4 cormidia (five replicates, total $N_{cormidia}$ = 89) was dissected off and transferred to a measuring cylinder filled with microfiltered sea water, and the vertical position of individual cormidia was recorded at the start of experiment (T_0), and after 24h. Our data (Table S5) document that within that period all cormidia became released, and all matured to eudoxids, simultaneously becoming buoyant. This further supports the notion that the process of cormidium release is not only an additional step in species sexual reproduction, but rather a mechanism of producing reproductively competent, and ecologically independent, individual-like organisms.

Despite these distributional differences, since eudoxids share morphological traits with cormidia still attached to the colony, their diets are likely similar. Feeding in most calycophoran siphonophores occurs through veronica movement (48) in which nectophores pump to swim in circles, while stem and tentacles extend forming a feeding spiral that maximizes prey capture area (Fig. 8F). To our surprise, we were able to document similar behavior in eudoxids (Fig. 8G, Movie S4-5), despite being achieved with a different toolset. We documented for the first time *Chelophyes appendiculata* eudoxids swimming in circles with gonophore pumping, simultaneously extending their tentacles, hence mimicking behavior of polygastric colonies.

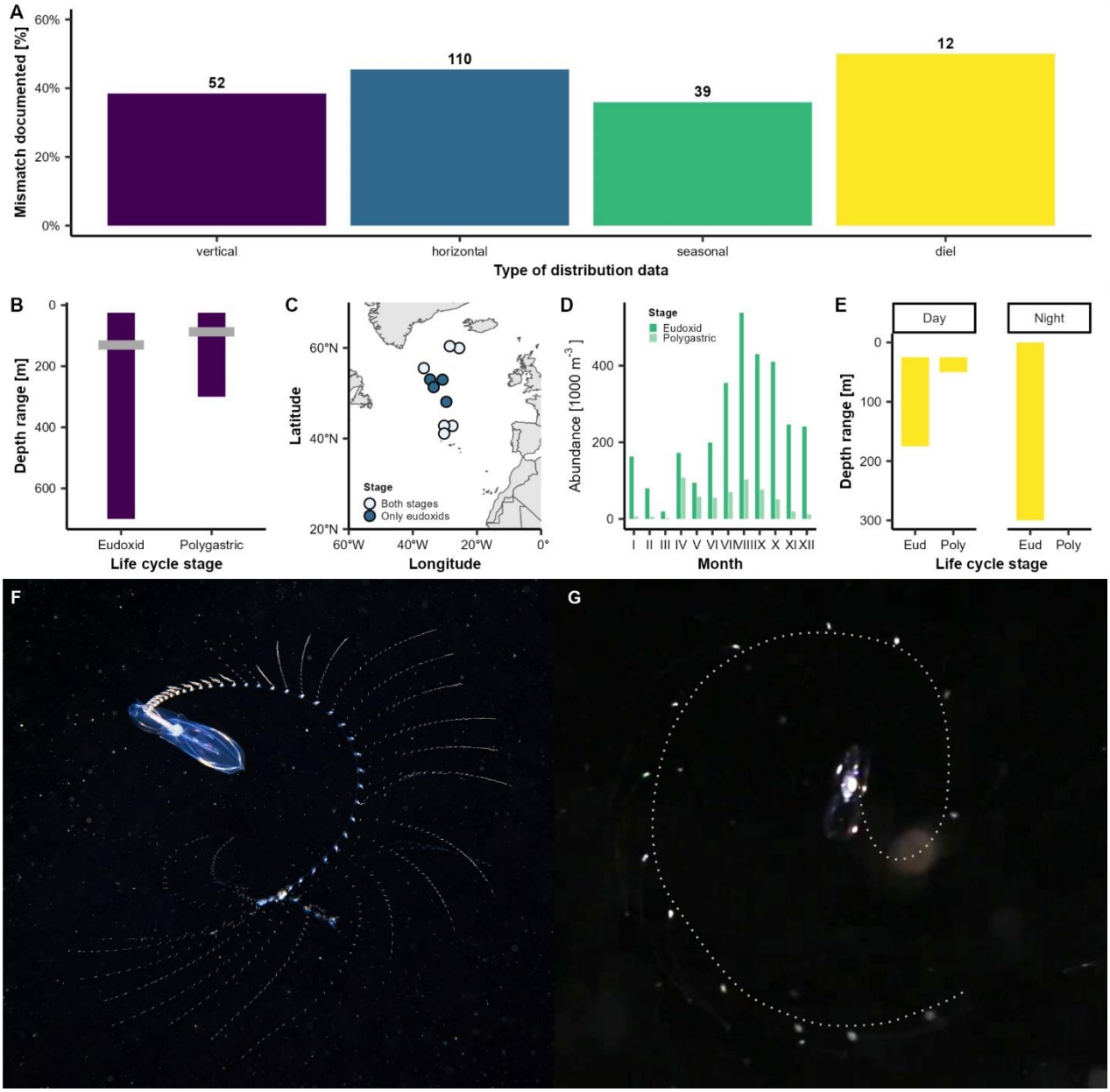

Figure 8. Ecological mismatch between eudoxid and polygastric life cycle stages. **A.** Results of literature review indicating percent of all references analyzed (numbers in bold; Data S2) containing evidence for distribution mismatch between two life cycle stages separated into four types of distributional data: vertical, horizontal, seasonal and diel. **B.** Example of vertical distribution mismatch in *Abylopsis tetragona*, based on data from (38), depicting depth ranges and mean distribution (grey line) of two life cycle stages. **C.** Example of horizontal distribution mismatch in *Chuniphyes multidentata*, based on data from (43), depicting sites where either both life cycle stages (light blue) or only eudoxids (dark blue) were present. **D.** Example of seasonal mismatch in eudoxid (dark green) and polygastric colonies (light green) of *Dimophyes arctica*, based on data from (45). **E.** Example of diel mismatch in distribution ranges of eudoxids (Eud) and polygastric colonies (Poly) in *Lensia cossack*, based on data from (38). **F.** Photograph of *Chelophyes appendiculata* performing veronica movement captured by Alexander Semenov (White Sea Biological Station). **G.** Frame grab from video (Movie S4) documenting *C. appendiculata* eudoxid performing veronica movement – dotted grey line indicates extent of eudoxid tentacle to facilitate interpretation.

Discussion

Here, we describe the acquisition of a unique evolutionary stage in the life cycles of colonial siphonophores, known as eudoxids. We provide evidence for the morphological integration of zooids within a eudoxid, an evolutionary trajectory marked by increasing integration and complexity reduction of zooids, and the acquisition of eudoxid-specific structures and processes (e.g., detachment ring, phyllocyst, post-release maturation). Additionally, we highlight the functional and physiological integration of eudoxids, distributional niche partitioning between life cycle stages, and the existence of complex behaviors resulting from the cooperative actions of zooids. Thus, we consider eudoxids to exhibit all hallmarks of individuality: cooperative, functional, and evolutionary (3, 30).

Evolution of siphonophore colony architecture and reproduction

The extreme complexity of siphonophore colonies arises through a highly regulated budding process, that in Codonophora starts with a primary bud, probud, that later subdivides into other zooids, forming a single cormidium (17). Sequential generation of new probuds results in the iterative, species-specific order in which zooids appear on a siphonophore stem, and renders full ontogeny of individual zooid types traceable along single colony stem. In agreement with Dunn and Wagner (17), we show that calycophoran cormidia are more modular than in other siphonophores, in that individual zooids are not dispersed along the stem, but rather remain clustered. Our data, however, indicate that *Chelophyes appendiculata* budding bypasses the probud subdivision, in that the original bud develops directly into a gastrozooid, while subsequent zooids are budded directly from gastrozooids' base (Fig. 2A). Alteration of probud subdivision might be a shared feature of Calycophorae, as it also seems to be the case in *Abylopsis tetragona* (49), *Sphaeronectes koelikeri* (50). Future exploration of cormidium budding across calycophorans, especially among "prayid" siphonophores, coupled with gene expression studies, will be necessary to better understand the fate of the probud in calycophorans and its evolution.

The apparent increase in cormidia modularity in Calycophorae coincided with the loss of their complexity (Fig. 2, 7). Calycophoran cormidia are deprived of palpons (except for *Stephanophyes superba*, 18), have only single gonophore per cormidium, but foremost have only a single bract or no bracts at all (Fig. 7, Data S1). We inferred a single acquisition of the eudoxid in calycophoran siphonophores, coinciding with the alteration to the bract morphology. This change involved twisting the bract attachment to the stem through the longitudinal canal lamella, resulting in the longitudinal canal becoming perpendicular to the stem (Fig. 7, Data S1). Given the likely muscular nature of these lamellae (e.g., 28, 51; Fig. 2C, 3E, 6C, Fig. S1), such repositioning might have secured a stronger attachment, necessary for mature eudoxid functioning and complex behavior (e.g., Fig. 8G). The subsequent evolutionary modifications of the bract included a reduction in the number of bracteal canal branches (Fig. 7, Data S1) leading to the retention of only the one forming the phyllocyst after cormidium detachment. Additionally, the acquisition of the capacity for remodeling was likely involved in the buoyancy maintenance of eudoxids (52; Fig. 5, 7, Table S5). Bracts are known to help maintain the buoyancy of siphonophores colonies (among other roles, 53). Despite the morphological diversity (e.g., 54) and abundance of bracts across siphonophore phylogeny, with only few losses, notably in the clade retrieved in our study comprising Clausophyidae + Hippopodidae (Fig. 7), their evolutionary nature remains elusive. Bracts have been suggested to be homologous to polyps (17-18) or medusae (21, 55). Although

our data did not resolve this long standing question, they do support the idea of the pivotal role of the bract in eudoxid formation.

Calycophoran eudoxids have been shown before to continue budding gonophores following cormidium detachment from the colony (56), and our data corroborates this ability (e.g., presence of secondary gonophore bud in Fig. 1C). These subsequent gonophores may either be of the same sex as the first one, or their sex may change (56), hence maximizing reproductive success. Sex determination in cnidarians is still poorly studied (57), but the process can be governed by either genetic (XY sex determination in *Hydractinia symbiolongicarpus*, 58) or environmental cues (temperature control in *Clytia* spp., 59). Intriguingly, colonies of *C. appendiculata* were shown to contain gonads of both sexes at the same time, when observed in the wild, but after maintenance in captivity, they became sequential hermaphrodites (59). The independence in budding subsequent reproductive structures supports our idea of the individual-like character of calycophoran eudoxids at the same time rendering them an interesting object for subsequent sex determination studies.

Mechanisms of siphonophore colony fragmentation

One of the unique features of clonal colonial taxa is their capacity to escape or delay senescence through repairing, replacing or removing malfunctioning modules (8, 60). Although the exact mechanisms may vary (e.g., 61), they appear to rely on a seemingly unpatterned distribution of colony modules that facilitates their replacement. However, the anterior-posterior patterning of the linear colonies in siphonophores, and their directional growth with strongly localized budding and stem cell populations (62), hampers module replacement and removal, as indicated by the limited regenerative potential of siphonophores (4, 48, 63).

One plausible outcome of the limited regenerative potential of siphonophores is the broad distribution of records of colony fragmentation across siphonophore phylogeny (Fig. 7, Data S1; 64). Some siphonophore colonies attain enormous lengths, particularly in apolemiid "physonects" (over 30 m, 28, 64) and "prayid" Calycophorae (45.7 m in *Praya dubia*, 65), and stem fragmentation was documented in these two groups (apolemiids – 66, "prayids" – 25; Data S1). These freely drifting stem fragments vary in length, module composition and reproductive capacity (e.g., 28, 66), indicating the unprogrammed nature of their separation, likely driven by the injury to the colony. Notably, stem-groups of certain "prayids" (e.g., Nectopyramidinae) often contain only single cormidium (25), but we do not consider them true eudoxids for the following reasons: i) their bracts do not form a phyllocyst nor ii) do they remodel, and iii) they do not resorb their stem, which can either remain unaltered (present on both anterior and posterior sides of the gastrozooid) or can expand near gastrozooid, forming the so-called central organ (18); more data are however needed, particularly on the fragmentation itself, to better support this classification. In contrast, we show here that colony fragmentation leading to eudoxid formation (i.e., cormidium release and eudoxid maturation) is a precisely timed process, relying on module (here cormidium) development (Fig. 4, Table S1-2) and loss of connectivity with the colony (Table S2).

The temporal and spatial separation of eudoxid and cormidium maturation, suggests presence of an inhibitory signal suppressing the bract remodeling, phyllocyst formation and stem resorption before cormidium release (Fig. 5). The nature of this signal remains to be determined, but our data on the detachment ring role in the cormidium release (Fig. 3A,

B, D) and on the cormidium release from stem fragments (Table S2), implies that it is the loss of connectivity with the colony that induces cormidium release and eudoxid maturation. It is likely, given the complex coordination system present in *C. appendiculata* and other siphonophores; 67-68), that sensing of cormidium integration with the colony (presence of connectivity) may involve the nervous system. We documented the existence of transverse neuronal bands in stems of *C. appendiculata* (Fig. 2A), that mirrored the position of detachment rings and remained connected with the two giant axons running along the entirety of the stem (Fig. 2A, Fig. S2A), supporting this claim. However, due to limited accessibility to fresh *C. appendiculata* colonies and inability to culture them, we were unable to design more complex experiments that would allow us to systematically test the role of the nervous system in this process. Alternatively, sensing of connectivity may be related to the flow in the stem (gastrovascular system; 67), food availability (e.g., fill level of lipid storage structure, the nectophore somatocyst) or a mix of above. Our observations on spatial distribution of the detachment rings (Fig. 4D) and their constriction prior to the detachment (Fig. 3), may indicate their role in limiting flow across the stem, a potential cue to start cormidium release. Interestingly, although we found detachment rings only in siphonophore species releasing eudoxids (Fig. 7), in non-Eudoxida we observed presence of transverse actin-rich bands in corresponding sites (Fig. 7), consistent with earlier studies (named collars, e.g., 51) that hypothesized their role in the control of local stem contractions (51). This may suggest that eudoxid-releasing calycophorans co-opted neuro-muscular toolkit present in other siphonophores, forming detachment rings that likely mediate intra-colony connectivity.

Role of muscles in eudoxid production

Through multiple lines of evidence (Fig. 4, 6), we found that cormidium release depends on muscle contraction of the detachment ring, likely a Eudoxida-unique structure (Fig. 7). Despite functional diversity of cnidarian muscles (reviewed in 69), information on their involvement in reproductive processes is scarce. Neuro-muscular control of zooid detachment was suggested during shedding of bracts and nectophores (51), as well as reproductive release of gonophores (28). Those three zooids share a similar structure of the actin-rich stem attachment at their base, called the lamella (also “autotomy joints”, 28, 51; Fig. 2C, 3E, 6C, Fig. S1), which could be contractile and participate in zooid detachment. Additionally, bud detachment in *Hydra* was shown to rely on actin dynamics and regionally-specific myosin phosphorylation for parent-bud boundary formation and detachment by constriction (70), and this resembles, to some extent, constriction-dependent eudoxid release (Fig. 4). We could show that eudoxid maturation is controlled by actomyosin (Fig. 6), reminiscent of the role of non-muscle myosin in the remodeling of regenerating *Clytia hemisphaerica* jellyfish (35) and in affecting growth of *Podocoryna carnea* stolons (71).

Life cycle complexity and species ecological success

A compelling picture emerges from our results on the ecological mismatches between eudoxids and polygastric colonies (Fig. 8, Data S2). This finding aligns with data from other marine taxa, which consistently show differences in habitat use, trophic modes and mobility across life stages in species with complex life cycles. Such variations are believed to underpin their ecological success (16, 72).

Fishing postures in siphonophores are closely related to their trophic niche (73). The so-called veronica movement, observed in both eudoxids and polygastric colonies (Fig. 8F,G), appears to be restricted to members of Eudoxida. In contrast, other siphonophores,

particularly those with longer and less contractile stems, adopt a “long-line” fishing posture (28, 73). Although there is currently no data on the trophic ecology of eudoxids, the presence of veronica movement in both life cycle stages of Eudoxida suggests that there may not be significant dietary differences between these stages. However, this hypothesis requires further investigation. The mechanisms underlying the acquisition and coordination of eudoxid behavioral complexity (e.g., Fig. 8G) remain to be determined. One intriguing possibility is that it involves nervous system rearrangement. Indeed we found that the two giant axons of the stem disappear during stem resorption (Fig. S2A, B). Should *C. appendiculata* become available in culture, the role of the nervous system in eudoxid behavior could be experimentally tested.

Study limitations

Our study did suffer from the inability to maintain long term culture *C. appendiculata*, which precluded us from obtaining more data, and designing more advanced experiments testing various aspects of eudoxid production. We also acknowledge that corroborating certain aspects of our phylogenetic reconstruction (Fig. 7, detachment ring acquisition in particular) will have to await broader taxon sampling, both for morphological examination and ideally phylogenomic analyzes. In addition, our review of the distribution mismatch between eudoxids and polygastric colonies was limited by the relatively low number of references distinguishing between abundances of the two life cycle stages, suggesting a need for increased resolution of abundance data in subsequent ecological works.

Materials and Methods

Ethics approval is not required for experimentation on cnidarians.

Collection and maintenance of *Chelophyes appendiculata*

Live specimens of *Chelophyes appendiculata* used in all experiments were collected in spring (2018-2022) from the Villefranche Bay (northern Mediterranean Sea), either in the vicinity of the Point B (43.6830 N, 7.3170 E) monitoring station or near the entrance of the bay. Sampling occurred in the early morning hours onboard RV Pelagia (Institute de la Mer de Villefranche-sur-Mer, France). To fish siphonophores, a plankton net (650 µm mesh) was dropped below the surface (1-2 m), and was slowly towed behind the vessel to avoid damage to specimens. Then, the cod-end was gently emptied into a 15L bucket (CAMBRO ®) prefilled with natural seawater. In case of large concentrations of plankton (e.g., during salp bloom) colonies of *C. appendiculata* were immediately transferred to a separate bucket with ladles.

After collection, specimens were moved to a temperature-controlled room (18°C) with a 12h:12h light cycle. Colonies designated for experiments were maintained unfed, in 15L buckets filled with filtered sea water, for no longer than 3 days. All other specimens (e.g., for immunostaining) were kept in 17L Kreisel tanks (Exotic Aquaculture) for 1-2 weeks, were fed daily with a mix of zooplankton, collected with 180 µm mesh plankton net from the Villefranche Bay and were starved only 1 day prior to use.

Initial processing of specimens

Specimens designated for subsequent analyzes were individually placed in a Petri dish coated with Sylgard 184 (Dow Corning Corporation) filled with microfiltered sea water (MFSW) and relaxed by dropwise addition of isotonic 7.5% solution of magnesium chloride hexahydrate in Mili-Q water at 1/3 MgCl2 to 2/3 MFSW ratio. As tentacles

tended to entangle and thus obscure observations, they were trimmed with an angled-micro knife (22.5°; Fine Science Tools GmbH). When stem fragments were needed, they were dissected from colonies also using angled micro-knife.

In vivo experiments

The following in vivo experiments were run on 1-day starved *C. appendiculata*: *Competence to release* (Table S1), *Stem fragmentation* (Table S2; Movie S1-3), *Buoyancy* (Table S6) and *Eudoxid behavior* (Movie S4-5). They were all run in a temperature controlled room (18°C).

Competence to release. Chelophyes appendiculata colonies (nectophore and entire stem) used were initially relaxed (as described above) in order to stage and photograph (NEX-5R Sony camera mounted on an Olympus SZ61 stereo-microscope) the most-posterior cormidium. To avoid specimen damage due to tentacle entanglement all tentacles were trimmed. After staging, colonies were transferred to one of two treatments: unperturbed or immobilized. In unperturbed treatment, specimens were transferred to 1L glass beakers filled with MFSW. In case of immobilized treatment, specimens were individually placed in Sylgard 184 coated Petri dish, prefilled with solution of 7.5% magnesium chloride hexahydrate in Mili-Q mixed with MFSW in 1:2. The anterior nectophore of a colony was then pinned down to Sylgard using ethanol-washed *Opuntia* spines. Usually three spines were used per nectophore, with one driven through nectophore tissues near the ostium, and two placed on both sides of the anterior tip of the nectophore, which successfully limited nectophore movement. Then, the magnesium chloride solution was gently replaced with MFSW with antibiotics (1/2000 dilution of a penicillin [10000 units stock] and streptomycin [10 mg per ml] solution; Sigma Aldrich, #P4333), which was replaced daily. The experiments were run for either 24h or 48h, with observations every 2-3h, except for nights. Upon every release event, the stage of released cormidium was noted down (Table S1).

Stem fragmentation. Stems of *C. appendiculata* colonies were relaxed and their tentacles trimmed as described above. They were then cut into 2-, 3- or 4-cormidia long stem fragments (once a single cormidium was dissected off, Movie S3), and the stage of development of individual cormidia was noted down. The fragments were then individually transferred either into 6-well plates or glass micro-chambers. In case of 6-well plates, they were prefilled with 6 ml of MFSW with antibiotics (as above; replenished daily), and fragments were observed Olympus SZ61 stereo-microscope with NEX-5R Sony camera at varying frequency (Table S2), with the picture taken at every time point and observations of cormidium release noted down. The glass micro-chambers were made by breaking glass microscope slides, and positioning resulting pieces in a Petri dish (3 cm diameter) to form a channel, roughly 1 mm in width. The chambers were then placed directly under Zeiss Axio Observer, prefilled with MFSW with antibiotics to the upper level of glass slide upper surface, and the stem fragment was put directly to the channel. The movement of the stem fragment within the channel was then constrained by placing *Opuntia* spines on either side of the channel. Zeiss's ZEN Microscopy Software, was then used to set automatic picture capture every 1 or 2 minutes, for about 24h, across the full z-extent of the channel. To minimize file size, these pictures were then exported as movies (Movie S1-S3) at high frames-per-second rating and at single z-plane, chosen based on stem fragment position throughout the experiment.

Buoyancy. Five experiments were run, each with a single *C. appendiculata* colony. Each colony was first relaxed (as described in the Initial processing of specimens section), all tentacles were trimmed, and a single stem fragment was dissected off that spanned all S3 cormidia. The stem fragment was then placed in a 50 ml measuring cylinder, prefilled with MFSW with antibiotics (as described above), and the position of cormidia was recorded as either laying on the bottom (0) or floating (1). Then the subsequent recording occurred after 24 h (Table S5).

Eudoxid behavior. Twenty eudoxids were taken from Kreisel tank where polygastric colonies were kept, and were transferred to a 1L rectangular tank filled with MFSW. Eudoxid behavior was recorded using Canon EOS 6D camera with Canon 100 mm f/2.8 L EF Macro IS USM lens (Movie S4-5).

Immunostaining and actin detection

Specimens designated for immunohistochemistry were processed as in Mańko et al. (19) using anti-tyrosinated tubulin antibody (YL1/2, 1:50, Abcam, #6160) and/or anti-FMRFamide antibody primary antibodies coupled with secondary antibodies, Alexa Fluor 488-conjugated phalloidin (1:50, solubilized in methanol; Thermo Fisher Scientific, #10125092), and Hoechst (Sigma Aldrich, #94403, 1/2000). Samples were gradually (10%-20%-40%) transferred to Citifluor AF-1 antifade mountant for imaging. Preparations were then visualized under Leica's SP5 and SP8 confocal microscopes. Given the large size of imaged animals, multiple tiles spanning all-z planes were often taken. These were automatically aligned using Leica Application Suite X Life Science Microscope software, while z-stacks were projected using standard deviation projection in ImageJ.

Pharmacological inhibition experiments

2- and 3-cormidia long stem fragments (Table S3) were individually transferred to 6-well plates prefilled with 10 ml of solutions corresponding to treatments analyzed. These included: 1 or 5 µM Blebbistatin (Sigma-Aldrich, #B0560; solution in MFSW, diluted from a 34 mM stock solution in DMSO); $MgCl_2$ (solution of 7.5% magnesium chloride hexahydrate in Mili-Q mixed with MFSW in 1:2 proportion); DMSO (1.47 µL DMSO in MFSW, corresponding to DMSO concentration in 5 µM blebbistatin treatment); MFSW. Experiments were run in temperature controlled conditions at 18°C, and antibiotics were added to each treatment as described above. The development stage of each cormidium was staged in each stem fragment analyzed and individually photographed either under Zeiss Axio Observer or using Sony camera (NEX-5R) mounted on an Olympus SZ61 stereo-microscope. They were imaged again after 22h and their phenotype was scored in the following categories: released cormidia (number of cormidia released from stem fragment); remodeled bracts (number of bracts that whose morphology matches that of released eudoxid bract); aberrant bract morphology (number of bracts whose morphology differs from that of eudoxid bract); aberrant bracteal canal (number of bracts showing alteration of bracteal canal morphology); stems resorbed (number of cormidia not showing signs of presence of loose stem).

Electron microscopy

Two samples (3-cormidia long stem fragment and two eudoxids of *C. appendiculata*) were preprocessed (relaxing and dissections) were preprocessed as described in Initial processing of specimens section. Specimens were then transferred separately to 1.5 ml Eppendorf tube and were fixed overnight at 4°C in a solution of 0.05M sodium cacodylate

buffer (pH 7.2-7.4), 0.025% $MgCl_2$, 2.5% glutaraldehyde, 0.8% paraformaldehyde and 4.45M NaCl in deionized water. Subsequent steps leading to resin embedding were carried out at the Plateforme Commune de Microscopie Electronique, Université Nice Côte d'Azur. Transmission electron microscopy images of ultra thin sections were acquired on Tecnai G2 Spirit BioTWIN (FEI) at 120 kV at the Electron Microscopy Section at the Faculty of Biology at the University of Gdańsk.

DNA Extraction & sequencing

DNA was extracted from nectophores or a portion of the siphosome stored in ethanol at -20°C. DNA was extracted using the DNeasy Blood & Tissue Kit (Qiagen), following kit instructions. As much ethanol was removed from samples as possible before adding buffer ATL. Samples were incubated at 56°C for 3 hours. PCR of 16S and 18S was done with the following primers (16S: SHA 5' ACGGAATGAACTCAAATCATGT 3', SHB 5' TCGACTGTTTACCAAAAACATA 3', 74; 18S MitchA 5' AACCTGGTTGATCCTGCCAGT 3', MitchB 5' TGATCCTTCTGCAGGTTCACCTAC 3', 75), using the Phusion high fidelity polymerase (New England Biolabs) and annealing temperatures of 50°C and 55°C respectively (for cycling profiles see 16S:33, 18S:76). PCR products were cleaned up using the QIAquick PCR Purification Kit (Qiagen) following kit instructions, and were sent to Eurofins Genomics GmbH (Germany) for Sanger sequencing. In addition to using the same forward and reverse PCR primers for sequencing, the following internal primers were used for 18S sequencing: 18SR1028 5'CTGCGAAAGCATTTGCCAAG 3' and 18SF970: 5'CTAGGACGGTATCTGATCGTCTTCG 3',77).

Phylogenetic analyses

Available 16S and 18S rDNA sequences of siphonophores were retrieved from NCBI, except for *Physophora gilmeri* and *Thermopalia taraxaca*, whose 18S sequences were partial, and *Rosacea flaccida* and *Gymnopraia lapislazula*, whose phylogenetic positions were poorly supported. Additionally, because the positions of *Cordagalma ordinatum* and *Frillagalma vityazi* in rDNA-based phylogenies (75, 78) were incongruent with those in phylogenomic-based phylogenies (36), these species were also excluded from the analyses. Four species included in the molecular phylogeny (*Dendrogramma enigmatica*, *Tottonophyes enigmatica*, *Sphaeronectes haddocki*, *and Sphaeronectes christiansonae*) were excluded from the analyses due to the lack of information about their eudoxids.

We added new sequences for 18 calycophoran species for both ribosomal markers, as well as the 18S of *Lilyopsis medusa*. The outgroup included five hydrozoan species: Ectopleura dumortieri, *Hydra circumcincta*, *Staurocladia wellingtoni*, *Porpita porpita*, and *Velella velella*. We aligned the sequences using MAFFT v7.271 L-INS-I algorithm (79) and conducted constrained and unconstrained Maximum Likelihood (ML) analyses on the concatenated 16S-18S alignment using IQTree with 1000 bootstrap replicate. ModelFinder implemented in IQTree v1.5.5. was used to assess the relative model fit, selecting GTR+R4 for having the lowest Bayesian Information Criterion score. The constrained tree topology was derived from Munro et al. (38; Fig. S5, Data S4).

A matrix including 26 morphological characters coded for all described siphonophore species was assembled from an extensive literature review (Data S1, S4). For each species included in the phylogeny, we first analyzed the original species description, and in case of absence of information on a given trait we subsequently checked information in morphological reviews (Table S1). We then encoded additional information stemming

from present work. The evolution of these characters was inferred by parsimony onto the ML phylogeny using Mesquite (80).

Siphonophore ecology review

Information on distribution mismatch between polygastric colonies and eudoxids were retrieved from a review of siphonophore reference database curated by late Philip R. Pugh (National Oceanographic Centre), including 1655 positions, spanning years 1725-2023. First, the type of each reference was verified and only scientific papers and books were retained, removing technical reports, regional species checklists, theses and grey literature. Then we inferred the field of study for each of those by analysis of the title and abstract, retaining only references containing information on species distribution (vertical, horizontal, seasonal or diel; N=520). We then verified if these contain information on distribution of Calycophorae, excluding references dealing either collectively with siphonophores, or not mentioning calycophores (N=386). From these we then kept only those that include information on eudoxids (N=122, Data S2), and these were then read thoroughly and checked for indication of distribution mismatch. Distribution was classified as pointing at mismatch when: for horizontal data, eudoxids present at sites when no polygastric stages were present, for vertical data, eudoxids showing different depth range or mean depth distribution than polygastric, for seasonal data, eudoxids not following seasonal abundance cycle of polygastric stages (e.g., presence in seasons when no or almost no polygastric stages were recorded), for diurnal data, eudoxids showing different vertical distribution between day and night as compared to polygastric stages. Example plots were generated using raw data provided in the papers (*Chuniphyes multidentata* horizontal distribution – 43, *Abylopsis tetragona* vertical and *Lensia cossack* diel distributions – 38) or data were retrieved through digitization of published plots using plotdigitzer.com (*Dimophyes arctica* seasonal distribution – 45).

References

1. L. W. Buss, *The Evolution of Individuality*. (Princeton University Press, Princeton 1987).
2. J. Maynard Smith, E. Szathmáry, *The Major Transitions In Evolution* (Oxford Univ. Press, 1995).
3. Y. Carmel, A. Shavit, Operationalizing evolutionary transitions in individuality. *Proc. R. Soc. B* **287**, 20192805 (2020)
4. G. O. Mackie, From aggregates to integrates: physiological aspects of modularity in colonial animals. *Philos T Roy Soc B* **313**, 175–196 (1986).
5. P. Cartwright, M. K. Travert, S. M. Sanders, The evolution and development of coloniality in hydrozoans. *J. Exp. Zool. (Mol. Dev. Evol.)* **336**, 293-299 (2021).
6. L. S. Hiebert, C. Simpson, S. Tiozzo, Coloniality, clonality, and modularity in animals: The elephant in the room. *J. Exp. Zool. Pt. B.* **336**, 198–211 (2021).
7. F. D. Brown, Evolution of animal coloniality and modularity: Emerging themes. *J. Exp. Zool. (Mol. Dev. Evol.)* **336**, 187–190 (2021)
8. M. Reichard, Evolutionary perspectives on ageing. *Semin. Cell. Dev. Biol.* **70**, 99–107 (2017).
9. C. Simpson, A. Herrera-Cubilla, J. B. C. Jackson, How colonial animals evolve. *Sci. Adv.* **6**, eaaw9530 (2020).

10. D. J. Ayre, T. P. Hughes, Genotypic diversity and gene flow in brooding and spawning corals along the Great Barrier Reef, Australia. *Evolution* **54**, 1590–1605 (2000).

11. T. Nakazawa, Ontogenetic niche shifts matter in community ecology: a review and future perspectives. *Pop. Ecol.* **57**, 347–354 (2015).

12. K. Wasson, A. T. Newberry. Modular metazoans: gonochoric, hermaphroditic, or both at once? *Invert. Rep. Dev,* **31**, 159–175 (1997).

13. J. R. Pannell, J. R. Auld, Y. Brandvain, M. Burd, J. W. Busch, P.-O. Cheptou, J. K. Conner, E. E. Goldberg, A.-G. Grant, D. L. Grossenbacher, S. M. Hovick, B. Igic, S. Kalisz, T. Petanidou, A. M. Randle, R. Rubio de Casas, A. Pauw, J. C. Vamosi, A. A. Winn (2015). The scope of Baker's law. *New Phytol.* **208**, 656–667 (2015)

14. A. L. Phillippi, P. O. Yund, Self-fertilization and inbreeding depression in three ascidian species that differ in genetic dispersal potential. *Mar. Biol.* **164**, 179 (2017).

15. B. J. Gemmell, J.O. Dabiri, S. P. Colin, J. H. Costello, J. P. Townsend, K. R. Sutherland, Cool your jets: biological jet propulsion in marine invertebrates. *J. Exp. Biol.* **224**, jeb222083 (2021).

16. M. Boosten, C. Sant, O. Da Silva, S. Chaffron, L. Guidi, L. Leclère Loss of the benthic life stage in Medusozoa and colonization of the open ocean. *biorxiv* 528668 (2023).

17. C. W. Dunn, G. P. Wagner, The evolution of colony-level development in the Siphonophora (Cnidaria:Hydrozoa). *Dev. Genes Evol.* **216**, 743–354 (2006).

18. A. K. Totton, H. E. Bargmann, *A Synopsis of the Siphonophora.* (Trustees of the British Museum (Natural History), London, 1965).

19. M. K. Mańko, C. Munro, L. Leclère, Establishing Bilateral Symmetry in Hydrozoan Planula Larvae, a Review of Siphonophore Early Development. *Integr. Comp. Biol.* **63**, 975–989 (2013).

20. C. Munro, Z. Vue, R. R. Behringer, C. Dunn, Morphology and development of the Portuguese man of war, Physalia physalis. *Sci. Rep.* **9**, 15522 (2019).

21. E. Haeckel, Report on the Siphonophorae collected by HMS Challenger during the years 1873-1876. *Report of the Scientific Results of the voyage of H.M.S. Challenger. Zoology* **28**, 1–380 (1888).

22. P. Schuchert , DNA barcoding of some Pandeidae species (Cnidaria, Hydrozoa, Anthoathecata). *Rev. Suisse Zool.* **125,** 101-127 (2018).

23. C. Gegenbaur, Beitrage zur naheren Kenntniss der Schwimmpolypen. (Siphonophoren.) *Z. wiss. Zool.* **5** (1853).

24. R. Leuckart, *Zoologische Untersuchungen. 1. Die Siphonophoren.* (Giessen 1853).

25. A. K. Totton, Siphonophora of the Indian Ocean together with systematic and biological notes on related specimens from other oceans. *Discovery Reports* **27**, 1–162 (1954).

26. M. M. Grossmann , D. J. Lindsay, A. G. Collins, The endo of an enigmatic taxon: Eudoxia macra is the eudoxid stage of *Lensia cossack* (Siphonophora, Cnidaria). *Syst. Biodiv.* **11**, 381-387 (2013).

27. D. S. Oderberg, Siphonophores a metaphysical case study, in A. S. Meincke, J. Dupré Eds., *Biological Identity* (Taylor and Francis, 2020)

28. G. O. Mackie, P. R. Pugh, J. E. Purcell, “Siphonophore Biology” in *Advances in Marine Biology*, J. H. S. Blaxter, A. J. Southward, Eds. (Academic Press, 1988) pp. 97–262.

29. G. O. Mackie, “Siphonophores, Bud Colonies, and Superorganism” in *The Lower Metazoa*, E. Dougherty, Ed. (University of California Press, Berkeley, 1963), pp. 329–337.

30. S. L. Diaz-Muñoz, A. M. Boddy, G. Dantas, C. M. Waters, J. L. Bronstein, Contextual organismality: Beyond pattern to process in the emergence of organisms. *Evolution* **70**, 2669–2677 (2021).

31. P.E. Müller 1871. *Iagttagelser over nogle Siphonophores*. (Jacob Lunds Boghandel Kjobenhavn, 1871).

32. J. E. Purcell, Feeding and growth of the siphonophore *Muggiaea atlantica* (Cunningham 1893). *J. Exp. Mar. Biol. Ecol.* **62**, 39-54 (1982).

33. P. Licandro, S. Souissi, F. Ibanez, C. Carré, Long-term variability and environmental preferences of calycophoran siphonophores in the Bay of Villefranche (north-western Mediterranean). *Prog. Ocean.* **97-100**, 152-163 (2012).

34. S. H. D. Haddock, C. W. Dunn, P. R. Pugh, A re-examination of siphonophore terminology and morphology, applied to the description of two new prayine species with remarkable bio-optical properties. *J. Mar. Biol. Assoc. UK* **85**, 695–708 (2005).

35. C. Sinigaglia, S. Peron, J. Eichelbrenner, S. Chevalier, J. Steger, C. Barreau, E. Houliston, L. Leclère, Pattern regulation in a regenerating jellyfish. *eLife* **9,** *e54868* (2020).

36. C. Munro, S. Siebert, F. Zapata, M. Howison, A. Damian-Serrano, S. H. Church, F. E. Goetz, P. R. Pugh, S. H. D. Haddock, C. W. Dunn, Improved phylogenetic resolution within Siphonophora (Cnidaria) with implications for trait evolution. *Mol. Phyl. Evol.* **127**, 823–833 (2018).

37. P. R. Pugh, C. W. Dunn, S. H. D. Haddock, Description of *Tottonophyes enigmatica* gen. nov., sp. nov. (Hydrozoa, Siphonophora, Calycophorae), with a reappraisal of the function and homology of nectophoral canals. *Zootaxa* **4415**, 452-472 (2018).

38. M. M. Grossmann, J. Nishikawa, D. J. Lindsay, Diversity and community structure of pelagic cnidarians in the Celebes and Sulu Seas, southeast Asian tropical marginal seas. *Deep-Sea Res. I: Oceanographic Research Papers* **100**, 54–63 (2015).

39. F. Pagès. F. Kurbjeweit Vertical distribution and abundance of mesoplanktonic medusae and siphonophores from the Weddell Sea, Antarctica. *Polar. Biol.* 14, 243-251 (1994).

40. P. R. Pugh, G. A. Boxshall 1984 The small-scale distribution of plankton at a shelf station off the northwest African coast. *Cont. Shelf Res.* **3**, 399-423 (1984).

41. P. R. Pugh, F. Pagès, B. Boorman, Vertical distribution and abundance of pelagic cnidarians in the eastern Weddell Sea, Antarctica. *J. Mar. Biol. Assoc. UK* **77**, 341–360 (1997).

42. K. Rengarajan, Quantitative and seasonal abundance of siphonophores along the southwest coast of India and the Laccadive Sea. *J. Mar. BioI. Ass. India* **25**, 17-40 (1983).

43. A. Hosia, L. Stemmann, M. Youngbluth, Distribution of net-collected planktonic cnidarians along the northern Mid-Atlantic Ridge and their associations with the main water masses. *Deep-Sea Research Part II: Topical Studies in Oceanography* **55**, 106–118 (2008)

44. A. Panasiuk, L. Grzonka, P. Prątnicka, J. Wawrzynek-Borejko, M. Szymelfening, Zonal variability of pelagic Siphonophora (Cnidaria) in the atlantic sector of the southern ocean. *J. Sea Res.* **165**, 101951 (2020).

45. A. Hosia, U. Båmstedt, Seasonal abundance and vertical distribution of siphonophores in western Norwegian fjords. *J. Plankton Res.* **30**, 951-962 (2008).

46. A. Hosia, T. Falkenhaug, E. J. Baxter, F. Pagès, Abundance, distribution and diversity of gelatinous predators along the northern Mid-Atlantic Ridge: A comparison of different sampling methodologies. *PLoS ONE* **12**, e0187491 (2017).

47. P. R. Pugh, Some observations on the vertical migration and geographical distribution of Siphonophores in the warm waters of the North Atlantic Ocean. in S.Z. Qasim Ed., *Proceedings of the Symposium on Warm Water Zooplankton* (Goa, National Institute of Oceanography, 1977), pp. 362-378.

48. G. O. Mackie, D. A. Boag, Fishing, feeding and digestion in siphonophores. *Pubblicazioni della Stazione Zoologica di Napoli* **33**, 178–96 (1963).

49. K. C. Schneider, Mittheilungen über Siphonophoren. II. Grundriss der organisation der Siphonophoren. (Jena) Zoologischen Jahrbücher. *Abteilung für Anatomie und Ontogenie der Tiere Abteilung für Anatomie und Ontogenie der Tiere* **9**, 571–664 (1896).

50. C. Chun, Ueber die cyclische Entwickelung der Siphonophoren. 2. *S.B. preuss. Akad. Wiss*. 511-529 (1885).

51. C. J. P. Grimmelikhuijzen, A. N. Spencer, D. Carré, Organization of the nervous system of physonectid siphonophores. *Cell Tissue Res.* **246**, 463–479 (1986).

52. R. R. Bidigare, D. C. Biggs, The role of sulfate exclusion in buoyancy maintenance by siphonophores and other oceanic gelatinous zooplankton. *Comp. Biochem. Physiol. A* **66**, 467–471 (1980).

53. W. Garstang, The morphology and relations of the Siphonophora. *Q. J. Microsc. Sci.* **87**, 103–193 (1946).

54. P. R. Pugh, A revision of the family Forskaliidae (Siphonophora, Physonectae). *J. Nat. Hist.* **37**, 1281–1327 (2003).

55. R. Woltereck, Beiträge zur Ontogenie und Ableitung des Siphonophorenstocks, mit einem Anhang zur Entwicklungsphysiologie der Agalmiden. *Zeitschrvt für Wissenschaftliche Zoologie* **82**, 611–637 (1905).

56. C. Carré, D. Carré, A complete life cycle of the calycophoran siphonophore *Muggiaea kochi (*Will) in the laboratory, under different temperature conditions: ecological implications. *Philosophical Transactions of the Royal Society of London. Series B, Biological sciences* **334**, 27–32 (1991).

57. S. Siebert, C. E. Juliano, Sex, polyps, and medusae: Determination and maintenance of sex in cnidarians. *Mol. Reprod. Dev.* **84**, 105–119 (2017).

58. R. Chen, S. M. Sanders, Z. Ma, J. Paschall, E. S. Chang, B. M. Riscoe, C. E. Schnitzler, A. D. Baxevanis, M. L. Nicotra, XY sex determination in a cnidarian. *BMC Biol* **21**, 32 (2023).

59. D. Carré, C. Carré, Origin of germ cells, sex determination, and sex inversion in medusae of the genus *Clytia* (Hydrozoa, Leptomedusae): The influence of temperature. *J. Exp. Zool.* **287**, 233–242 (2000).

60. J. W. Vaupel, A. Baudisch, M. Dölling, D. A. Roach, J. Gampe, The case for negative senescence. *Theor. PopUL. Biol.* **65**, 339-351 (2004).

61. R. J. Lauzon, S. J. Kidder, P. Long, Suppression of programmed cell death regulates the cyclical degeneration of organs in a colonial urochordate. *Dev. Biol.* **301**, 92-105 (2007).

62. S. Siebert, F. E. Goetz, S. H. Church, P. Bhattacharyya, F. Zapata, S. H. D. Haddock, C. W. Dunn, Stem cells in *Nanomia bijuga* (Siphonophora), a colonial animal with localized growth zones. *EvoDevo* **6**, 22 (2015).

63. F. Moser, Die Siphonophoren der Deutschen Siidpolar Expedition, 1901-3. *Dtsch. Sudpol. Exped*. **12**,1-541 (1925).

64. S. Siebert, P. R. Pugh, S. H. D. Haddock, C. W. Dunn, Re-evaluation of characters in Apolemiidae (Siphonophora), with description of two new species from Monterey Bay, California. *Zootaxa* **3702**, 201–232 (2013)

65. C. R. McClain, T. J. Webb, N. A. Heim, M. L. Knope, P. M. Monarrez, J. L. Payne, Navigating uncertainty in maximum body size in marine Metazoans. *Ecol. Evol.* **14**, e11506 (2024)

66. K. Hiscock, G.M. Mapstone, D. V. P. Conway, N. Halliday, Occurrence of the physonect siphonophore *Apolemia uvaria* off Plymouth and in south-west England. *Mar. Biodiv. Rec.* **3**, e25 (2010).

67. G. O. Mackie, Coordinated Behavior in Hydrozoan Colonies in *Animal colonies Development and Function Through Time*, R. S. Boardman, A. H. Cheetham, W.A. Oliver J., Eds. (Dowden, Hutchinson and Ross, Pennsylvania, 1973).

68. G. O. Mackie, D. Carré, Coordination in a diphyid siphonophore. *Mar. Behav. Physiol.* **9**, 139-170 (1983).

69. L. Leclère, E. Röttinger, Diversity of Cnidarian Muscles: Function, Anatomy, Development and Regeneration. *Front. Cell Dev. Biol.* **4** (2017).

70. O. Holz, D. Apel, P. Steinmetz, E. Lange, S. Hopfenmüller, K. Ohler, S. Sudhop, M. Hassel, Bud detachment in Hydra requires activation of fibroblast growth factor receptor and a Rho–ROCK–Myosin II signaling pathway to ensure formation of a basal constriction. *Dev. Dyn.* **246**, 502-516 (2017).

71. N. Connally, C.P. Anderson, J.E. Bolton, E. W. Bolton, L. Buss, The Selective Myosin II Inhibitor Blebbistatin Reversibly Eliminates Gastrovascular Flow and Stolon Tip Pulsations in the Colonial Hydroid *Podocoryna carnea*. *PLoS ONE* **10**, e0143564 (2015).

72. D. J. Marshall, T. Connallon, Carry-over effects and fitness trade-offs in marine life histories: The costs of complexity for adaptation. *Evol. Appl.* **16**, 474–485 (2022).

73. D. C. Biggs, Field studies of fishing, feeding, and digestion in siphonophores. *Mar. Behav. Physiol.* **4 ,** 261-274 (1977).

74. Cunningham, L. Buss, Molecular evidence for multiple episodes of paedomorphosis in the family Hydractiniidae. *Biochem. Syst. Ecol*. **21**, 57–69 (1983).

75. L. Medlin, H. J. Elwood, S. Stickel, M. L. Sogin. 1988. The characterization of enzymatically amplified eukaryotic 16S-like rRNA-coding regions. *Gene* **71**, 491–499 (1988).

76. C. W. Dunn, P. R. Pugh, S. H. D. Haddock, Molecular Phylogenetics of the Siphonophora (Cnidaria), with Implications for the Evolution of Functional Specialization. *Syst. Biol.* **54**, 916–935 (2005).

77. L. Leclère, P. Schuchert, C. Craud, A. Couloux, M. Manuel, Molecular Phylogenetics of Thecata (Hydrozoa, Cnidaria) Reveals Long-Term Maintenance of Life History Traits despite High Frequency of Recent Character Changes. *Syst. Biol.* **58:** 509-526 (2009).

78. A. Damian-Serrano, S.H.D. Haddock, C. W. Dunn, The evolution of siphonophore tentilla for specialized prey capture in the open ocean. *PNAS* **118**, e2005063118 (2021).

79. K. Katoh, K. Misawa, K. Kuma, T. Miyata, MAFFT: a novel method for rapid multiple sequence alignment based on fast Fourier transform. *Nucleic Acids Res* **15**, 3059-3066 (2002).

80. W. P. Maddison, D.R. Maddison, Mesquite: a modular system for evolutionary analysis. Version 3.81. (2023).

Acknowledgments

We would like to thank numerous people who have made this work possible, by assisting us in sampling in the Villefranche Bay (Alexandre Alié, Institut de la Mer de Villefranche (IMEV), Alexandre Jan, University of Bergen), aiding in *C. appendiculata* maintenance (Alexandre Jan, University of Bergen), helping with confocal (Sébastien Schaub, IMEV; Michał Rychłowski, University of Gdańsk) and electron microscopy (Bastien Salmon, BIOM; Sophie Pagnotta, Université Nice Côte d'Azur; Dorota Łuszczek and Magdalena Narajczyk, University of Gdańsk), and to Alexander Semenov (White Sea Biological Station) for providing us with his photograph of *C. appendiculata* and Samuel Church (Yale University) for commenting on earlier version of manuscript. MKM also thanks Steven Haddock (Monterey Bay Aquarium Research Institute) for the invitation to join research cruise to Central Pacific, where some of the calycophores were sampled, and the Laboratoire de Biologie du Développement at the (IMEV), Clytia team in particular, for their hospitality during his numerous visits. We are grateful to the Imaging Platform (PIM), animal facility (CRB) and sailors (Jean-Yves Carval, in particular) of the IMEV, which is supported by EMBRC-France, whose French state funds are managed by the ANR within the Investments of the Future program under reference ANR-10-INBS-0, for continuous support.

Funding:

National Science Centre in Poland, Preludium 15, 2018/29/N/NZ8/01305 (MKM, LL)
University of Gdańsk, UGrant-START 533-O000-GS10-23 (MKM)
European Marine Biology Resource Centre, ACCESS, OOV–EMBRC FR–AAP2018–2180 (MKM, LL)

Author contributions:

Conceptualization: M.K.M., L.L.
Methodology: M.K.M., L.L.
Investigation: M.K.M., L.L., C.M.
Formal analysis: M.K.M., L.L.,
Funding acquisition: M.K.M., L.L.,
Visualization: M.K.M.
Writing - Original Draft: M.K.M
Writing - Review & Editing: L.L., C.M.
Supervision: L.L.

Competing interests: The authors declare that they have no competing interests

Data and materials availability:

All data needed to evaluate the conclusions in the paper are present in the paper and/or the Supplementary Materials